PLOS ONE

RESEARCH ARTICLE

An HDAC9-associated immune-related signature predicts bladder cancer prognosis

Yang Fu[1], Shanshan Sun[2], Jianbin Bi[1], Chuize Kong[1], Du Shi[1]*

1 Department of Urology, The First Hospital of China Medical University, Shenyang, PR China,
2 Department of Pharmacy, People's Hospital Affiliated of China Medical University, Shenyang, PR China

* shidu_cmu@163.com

OPEN ACCESS

Citation: Fu Y, Sun S, Bi J, Kong C, Shi D (2022) An HDAC9-associated immune-related signature predicts bladder cancer prognosis. PLoS ONE 17(3): e0264527. https://doi.org/10.1371/journal.pone.0264527

Editor: Jung Weon Lee, Seoul National University College of Pharmacy, REPUBLIC OF KOREA

Received: July 19, 2021

Accepted: February 12, 2022

Published: March 3, 2022

Data Availability Statement: All files are available from the TCGA (https://portal.gdc.cancer.gov/) and GEO database (accession number GSE32548, https://www.ncbi.nlm.nih.gov/geo/).

Funding: Prof.Chuize Kong received all the award. This work was supported by the Project of Liaoning Distinguished Professor [Grant No. [2012]145], China Medical University's 2017 Discipline Promotion Program [Grant No. 3110117040], the Shenyang Plan Project of Science and Technology [Grant No. F17-230-9-08], China Medical University's 2018 Discipline Promotion Program,

Abstract

Background

The close relationship between histone deacetylase 9 (HDAC9) and immunity has attracted attention. We constructed an immune signature for HDAC9, a vital epigenetic modification, to predict the survival status and treatment benefits in bladder cancer (BC).

Methods

An exhaustive analysis of HDAC9 and immunology via the tumor and immune system interaction database (TISIDB) was performed, and an immune prognostic risk signature was developed based on genes enriched in the top five immune-related pathways under high HDAC9 status. Comprehensive analysis of survival curves and Cox regression were used to estimate the effectiveness of the risk signature. The relationship between immunological characteristics and the risk score was evaluated, and the mechanisms were also explored.

Results

In the TISIDB, HDAC9 was closely related to various immunological characteristics. The risk signature was obtained based on genes related to prognosis enriched in the top five immune-related pathways under high HDAC9 status. The survival rate of the high-risk BC patients was poor. The risk score was closely related to multiple immunological characteristics, drug sensitivity, immunotherapy benefits and biofunctions.

Conclusion

An immune-related prognostic signature established for HDAC9 expression status could independently predict the prognosis of BC patients. The use of this signature could help clinicians make personalized treatment decisions.

and the 2017 National Key R&D Program Key Projects of Precision Medical Research [No. 2017YFC0908000]. The funder participated in the conceptualization, methodology, data curation, formal analysis, project administration, writing of original draft.

Competing interests: The authors have declared that no competing interests exist.

Background

As the most common urinary tumor in the whole world, the morbidity of bladder cancer (BC) is increasing each year in China [1]. Once BC progresses to the advanced stage of metastasis, conventional treatments are no longer effective [2, 3]. Furthermore, the clinical outcome of BC in the past few years has been poor because of high recurrence and drug resistance rates [4]. Thus, identifying new markers for prognosis and treatment for BC is necessary.

Histone deacetylation is considered a vital epigenetic modification in vivo. Histone deacetylases (HDACs) restrain related gene expression by catalyzing the deacetylation of histones or nonhistone proteins [5–7]. Histone deacetylase 9 (HDAC9) is a IIa HDAC subtype that has shown dual roles in tumors in multiple studies. In pancreatic ductal adenocarcinoma, high HDAC9 expression was significantly related to poor prognosis [8], and overexpression of HDAC9 promoted progression of the malignant phenotype of oral squamous cell carcinoma [9]. Additionally, elevated HDAC9 expression activated angiogenesis and invasion in triple-negative breast cancer [10]. However, HDAC9 also exhibited inhibitory effects in tumors. HDAC9 stimulated the expression of the ATDC target gene P53 by inhibiting ATDC expression, leading to inhibition of tumorigenesis [11], and it suppressed the proliferation of gastric cancer cells and enhanced sensitivity to cisplatin [12]. Our previous study suggested that low HDAC9 expression might facilitate clear cell renal cell carcinoma (ccRCC) cell growth, and we further found that HDAC9 was closely related to immunity and increased the infiltration levels of a variety of immune cells [13]. Other studies have revealed that HDAC9 deficiency significantly suppresses the immune response and inflammatory response [14–16]. Currently, immunotherapy has great potential in BC, and several immune-related drugs are currently in development [17]. Therefore, we sought to explore the pathogenesis of HDAC9 in BC, especially the relationship between HDAC9 and immunological characteristics.

In this study, a comprehensive analysis of HDAC9 was carried out to explore the connection between HDAC9 and the immune phenotype in BC. Importantly, we constructed an immune signature according to the expression status of HDAC9, a vital epigenetic modification, to predict the survival status and treatment benefits in BC.

Methods

Data acquisition from multiple public databases

The mRNA and clinically related factor data were obtained from The Cancer Genome Atlas (TCGA) database (https://portal.gdc.cancer.gov/), GSE32548 from the Gene Expression Omnibus (GEO) database (https://www.ncbi.nlm.nih.gov/geo/) and the IMvigor210 trial [18]. TCGA data comprised the training cohort, GEO data were used as the validation cohort, and IMvigor210 trial data were used to evaluate the effect of immunotherapy. Immunohistochemical images of HDAC9 in BC samples and normal samples were retrieved from the Human Protein Atlas (HPA) database (https://www.proteinatlas.org/). The HDAC9 antibody product number used on the HPA website was HPA028926 (Atlas Inc., Stockholm, Sweden). Then, the connections between HDAC9 and the immune phenotypes were studied via the tumor and immune system interaction database (TISIDB) (http://cis.hku.hk/TISIDB/index.php) [19].

Gene set enrichment analysis (GSEA)

BC samples in the TCGA database were split into two groups: a high HDAC9 expression group and a low HDAC9 group. Immune-related biological pathways were distinguished via GSEA through a "c5.all.v7.4.symbols.gmt" gene set downloaded from the Molecular Signatures Database (MSigDB). A nominal P value (NOM P value) < 0.05 and a false discovery rate Q

value (FDR Q value) < 0.25 were considered to indicate significant enrichment, and genes in the top five enriched immune-related biological pathways were extracted.

Risk score calculation

Genes related to survival were distinguished via univariable Cox regression. The P value was corrected for multiple comparisons by the FDR method, and a P adjusted value (P. adj) < 0.05 was considered statistically significant. Then, through least absolute shrinkage and selection operator (LASSO) Cox regression (the glmnet package of R), a risk score was calculated. The BC samples were split into two risk groups (low-risk vs. high-risk). A receiver operating characteristic (ROC) curve was utilized to analyze the risk signature accuracy for predicting prognosis via the R timeROC package, and the overall survival (OS) of the two groups was compared via a survival curve using the R survival package. To assess the ability of the risk score to independently predict prognosis, Cox regressions were then performed. The performance of prognosis prediction was also assessed through a nomogram and calibrations via the rms R package. To compare the predictive ability of our risk signature to other published signatures, we included risk signatures based only on prognostic-related genes [20–23] and those based on other risk factors [24–28] in the comparison of the AUCs of the ROC curves via the timeROC R package.

Coexpression analysis

Coexpression analysis was performed to further understand connections between HDAC9 and the risk score genes via the psych package of R. The relevant results were visualized using the ggplot2 R package. The P value was corrected for multiple comparisons by the FDR method, and P. adj < 0.05 was considered statistically significant.

The infiltration of immune cells and the risk score

To appraise the immune infiltration levels between two different risk groups, cell-type identification by estimating relative subsets of RNA transcripts (CIBERSORT) was carried out. In a previous study, CIBERSORT could calculate the relative abundance of 22 immune cells using transcriptome data [29].

Tumor microenvironment (TME) and the risk score

The infiltration of stromal cells (also called stromal score), infiltration of immune cells (also called immune score) and tumor purity are considered important indicators of the TME, and these aspects were assessed via Estimation of Stromal and Immune cells in Malignant Tumor tissues using Expression data (ESTIMATE) [30]. Relationships between the ESTIMATE results and the risk score were then assessed. The scores of 13 specific stromal cells in BC patients from TCGA were also calculated by the xCell package of R software [31] and the relationships between the xCell results and the risk score were also evaluated. In addition, the connections between genes included in the risk signature and TME related parameters (including stromal cells, immune cells, stromal score, immune score and tumor purity) were also explored via the psych R package (the P value was corrected for multiple comparisons by the FDR method, and P. adj < 0.05 was considered statistically significant.). The above relevant results were visualized using the ggplot2 R package.

The drug sensitivity and risk score

The connections between the half-maximal inhibitory concentration (IC50) of six common chemotherapy drugs (cisplatin, docetaxel, methotrexate, gemcitabine, paclitaxel and doxorubicin) and the risk score were explored using the pRRophetic R package [32]. As responses, including stable disease (SD), progressive disease (PD), complete response (CR) and partial response (PR), of each BC case to anti-PD-1 therapy were included in the IMvigor210 trial data, the effects of immunotherapy in the two risk groups were also analyzed.

Functional assessment of the risk score

To explore the risk score-related biological functions, GSEA was performed. The "c2.cp.kegg.v7.4.symbols.gmt" gene set and "c5.all.v7.4.symbols.gmt" gene set of the MSigDB database were downloaded. NOM P value < 0.05 and FDR Q value < 0.25 were considered significant.

Statistical analysis

The Wilcoxon rank sum test was used to compare the significant differences between the two groups. Log-rank analysis (survival curve) was utilized for survival analysis, correlation analysis was performed with the Spearman test, and the chi-square test was used to assess differences in the responses of the two groups of patients to immunotherapy. The non-parametric test was performed to compare differences between AUCs of the ROC curves also via the timeROC R package [33]. All statistical calculations were performed via R software (version 4.1.1).

Results

Preliminary exploration of HDAC9 in BC

We included 411 tumor samples and 19 normal samples from TCGA, of which clinical information was available for 409 samples (Table 1). Compared with normal bladder tissues, HDAC9 was found to be lower in tumor tissues according to TCGA (Fig 1A) and HPA (Fig 1B and 1C) data. It was worth noting that the significance level of the relationship between HDAC9 expression and immune subtypes in the BC ranked second among all tumors (Fig 1D and 1E) [34]. HDAC9 was also closely related to various immunological characteristics [including tumor-infiltrating lymphocytes (TILs) (S1A–S1F Fig), immunosuppressive cytokines (S2A–S2F Fig), immune-activating cytokines (S3A–S3F Fig), and major histocompatibility complex (MHC) molecules (S4A–S4F Fig), all figures were downloaded directly from the TISIDB.]. NK T cells (TILs), PDCD1LG2 (immunosuppressive cytokines), ICOS (immune-activating cytokines) and HLA-DOB (MHC molecules) were the most positively correlated with HDAC9 expression.

Establishment of the risk signature

According to the top five immune-related pathways in the GSEA results, HDAC9 played both immunosuppressive and immune activation effects in BC (Table 2). In total, 593 genes in the five pathways were extracted, and genes related to survival (P. adj < 0.05) were identified via univariable Cox regression (S1 Table). Then, through LASSO Cox regression, a risk score was calculated. (Fig 2A and 2B) (S2 Table). The survival rate of the high-risk BC patients was lower than that of the low-risk patients ($P < 0.001$) (Fig 2C). The areas under the curve (AUCs) were 0.812 (1 year), 0.809 (3 years) and 0.813 (5 years), and the C index was 0.780 (Fig 2D). The GSE32548 cohort, including 130 BC tissues and corresponding clinical data, was used to validate the signature (Fig 2E and 2F) (Table 3). The survival rate of the high-risk BC patients was

Table 1. Characteristics of the BC patients obtained from the TCGA database.

Basic information		TCGA (n = 409)
Age		69 (median)
Gender	Female	106
	Male	303
Grade	High	385
	Low	21
	Unknow	3
Stage	I & II	132
	III & IV	275
	Unknow	2
T classification		124
	T3 & T4	253
	TX	1
	Unknow	31
N classification	N0	237
	N1 &N2 & N3	131
	NX	36
	Unknow	5
M classification	M0	194
	M1	11
	MX	202
	Unknow	2

BC, bladder cancer; TCGA, the The Cancer Genome Atlas.

https://doi.org/10.1371/journal.pone.0264527.t001

also lower (P = 0.009) (Fig 2G), with AUCs of 0.858 (1 year), 0.781 (3 years) and 0.786 (5 years) and a C index of 0.895 (Fig 2H).

In the TCGA cohort, univariate Cox regression suggested that clinical stage, T stage, N stage and the risk score were significantly related to poor prognosis (Fig 3A) (all P values < 0.05), and the risk score could be considered a prognostic factor based on multivariate Cox regression (Fig 3B). In the GSE32548 cohort, univariate Cox regression revealed that T stage, grade and risk score were closely related to poor prognosis in BC (all P values < 0.05) (Fig 3C), and the risk score was also identified as a prognostic factor based on multivariate Cox regression (Fig 3D). Additionally, the nomogram and calibration curves appropriately predicted 1-year, 3-year and 5-year OS for both TCGA (Fig 4A–4D) and GSE32548 (Fig 5A–5D). Upon comparison with other signatures constructed through only prognosis-related genes (Fig 6A–6C) or other risk factors (Fig 6D–6F), our risk signature was found to be superior (Tables 4 and 5).

The relationships between HDAC9 and selected genes were assessed by coexpression analysis (S5 Fig). CDK6 was identified as the most positively correlated with HDAC9 expression, whereas NR1H2 was the most negatively correlated with HDAC9 expression.

The risk score was related to infiltration of various immune cells

The results of CIBERSORT revealed enrichment for signatures of M0 (Fig 7A) and M2 macrophages (Fig 7B) and neutrophils (Fig 7C) in high-risk BC patients (all P values < 0.05). Conversely, signatures of CD8 T cells (Fig 7D), activated memory CD4 T cells (Fig 7E), activated

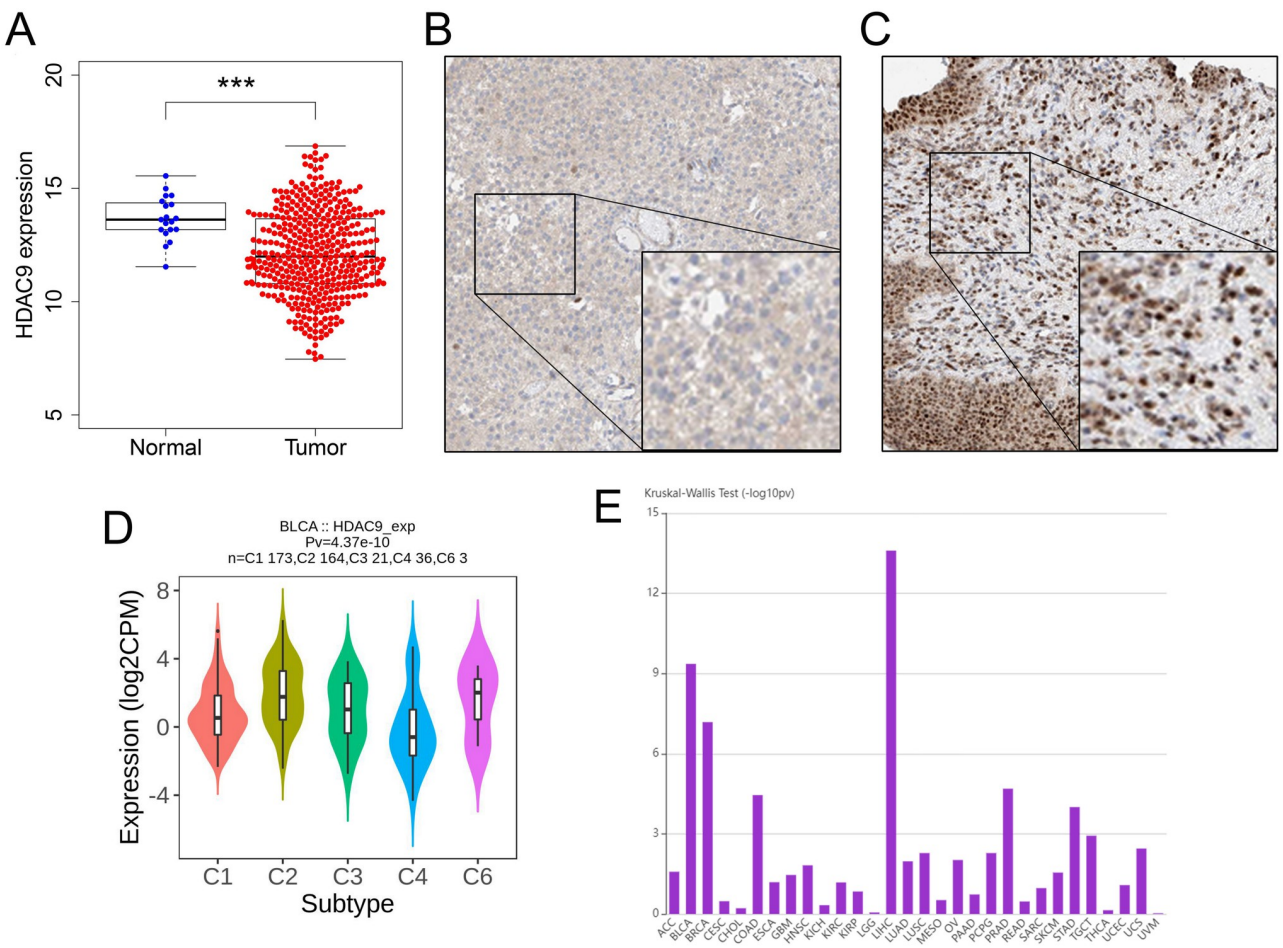

Fig 1. Preliminary exploration of HDAC9. According to TCGA data, low expression of HDAC9 was found in tumor samples (A). According to HPA data, lower expression of HDAC9 was found in tumor samples (B) than in normal samples (C). There was a significant difference between HDAC9 expression and immune subtype (D). It was worth noting that the significance level of the relationship between HDAC9 expression and immune subtypes in the BC ranked second among all tumors (E). HDAC9, histone deacetylase 9; TCGA, The Cancer Genome Atlas; HPA, Human Protein Atlas; BC, bladder cancer; C1, wound healing; C2, IFN-gamma dominant; C3, inflammatory; C4, lymphocyte depleted; C6, TGF-b dominant; ***, $P < 0.001$.

https://doi.org/10.1371/journal.pone.0264527.g001

Table 2. Gene sets enriched in the high HDAC9 phenotype via GO.

Gene set name	NES	NOM *p*-val	FDR *q*-val
GO_NEGATIVE_REGULATION_OF_IMMUNE_SYSTEM_PROCESS	2.356	0.000	0.000
GO_POSITIVE_REGULATION_OF_IMMUNE_EFFECTOR_PROCESS	2.297	0.000	0.000
GO_NEGATIVE_REGULATION_OF_IMMUNE_EFFECTOR_PROCESS	2.275	0.000	0.000
GO_NEGATIVE_REGULATION_OF_IMMUNE_RESPONSE	2.275	0.000	0.000
GO_B_CELL_ACTIVATION_INVOLVED_IN_IMMUNE_RESPONSE	2.255	0.000	0.000

HDAC9, histone deacetylase 9; GO, Gene Ontology; NES: normalized enrichment score; NOM: nominal; FDR: false discovery rate.
Gene sets with NOM *p*-val < 0.05 and FDR *q*-val < 0.25 were considered significant.

https://doi.org/10.1371/journal.pone.0264527.t002

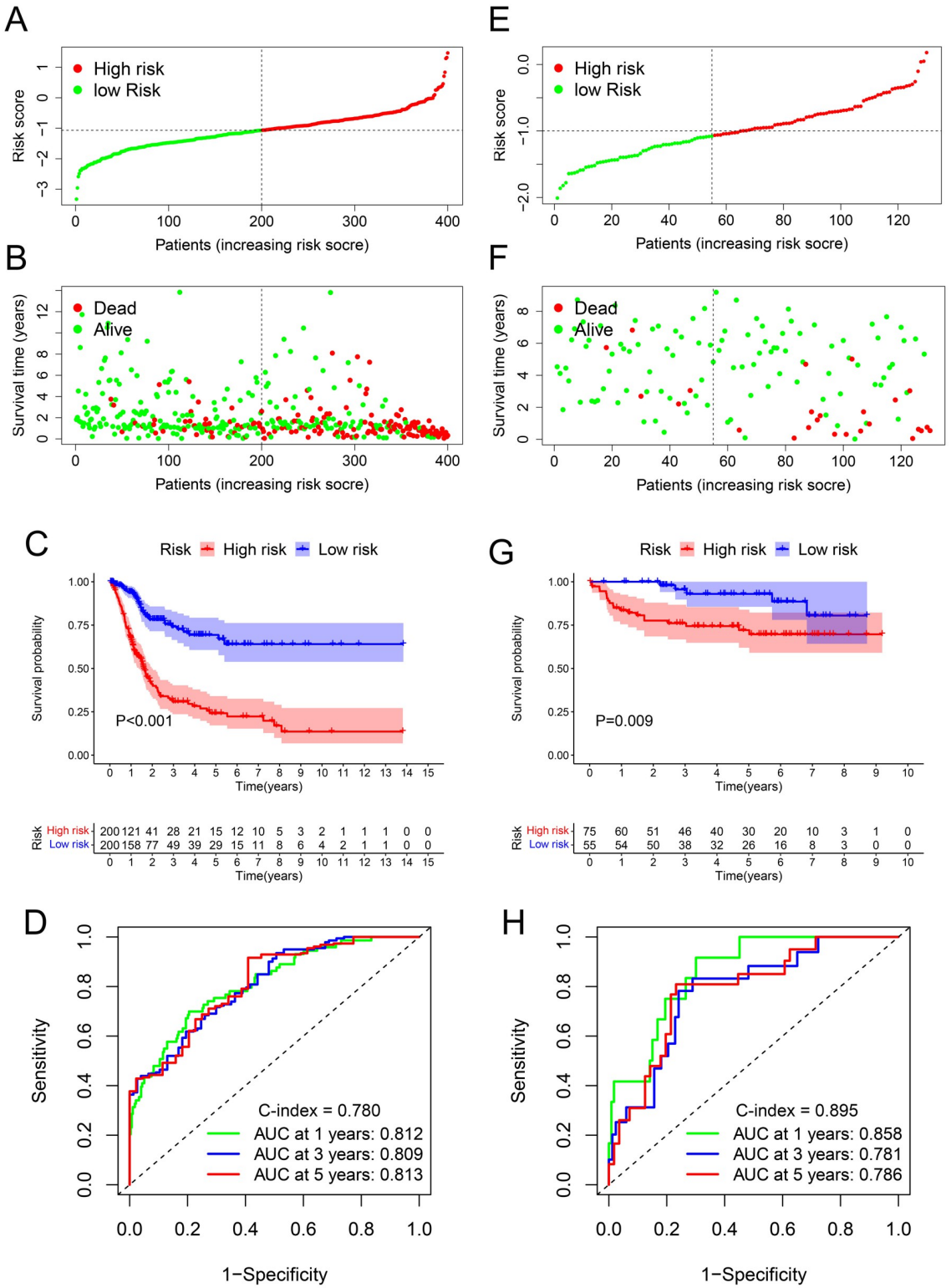

Fig 2. Establishment of the risk score. In the TCGA cohort, BC patients were distributed into different risk groups (A). Survival status of BC patients in different risk groups (B). The survival rate of the high-risk BC patients was worse than that of the low-risk patients (C). AUCs of the ROC curves were shown (D). In the verification cohort of the GEO, BC patients were distributed into different risk groups (E). Survival status of BC patients in different risk groups (F). The survival rate of the high-risk BC patients was worse than that of the low-risk patients (G). AUCs of the ROC curves were shown (H) TCGA, the Cancer Genome Atlas; GEO, Gene

Expression Omnibus; AUC, area under the ROC curve; OS, overall survival; ROC, receiver operating characteristics; BC, bladder cancer.

https://doi.org/10.1371/journal.pone.0264527.g002

dendritic cells (Fig 7F), follicular helper T cells (Fig 7G) and plasma cells (Fig 7H) were enriched in low-risk BC patients (all P values < 0.05).

The risk score could affect the change of TME

The relationship between the TME (including stromal score, immune score and tumor purity) and the risk score was also evaluated. The results revealed that the stromal score was positively correlated with the risk score (Fig 8A), but tumor purity was negatively correlated (Fig 8B) (all P values < 0.05). Nevertheless, there was no significant difference between the immune score and risk score (Fig 8C). In addition, signatures of adipocytes (Fig 9A), chondrocytes (Fig 9B), endothelial cells (Fig 9C), fibroblasts (Fig 9D), lymphatic endothelial cells (ly endothelial cells) (Fig 9E), mesenchymal stem cells (MSCs) (Fig 9F), myocytes (Fig 9G), and smooth muscle (Fig 9H) were enriched in high-risk BC patients (all P. adj < 0.05). Besides, the connections between genes included in the risk signature and TME related parameters (including stromal cells, immune cells, stromal score, immune score and tumor purity) were also explored and visualized via a heatmap (S6 Fig).

Risk score and drug sensitivity

We predicted the IC50 of six common chemotherapy drugs in the different groups. Cisplatin (Fig 10A) and docetaxel (Fig 10B) exhibited higher IC50 values in low-risk patients; thus, the high-risk group was more sensitive to cisplatin and docetaxel (all $P < 0.05$). Methotrexate (Fig 10C) and gemcitabine (Fig 10D) exhibited a higher IC50 in high-risk BC patients; thus, low-risk BC patients were more sensitive to methotrexate and gemcitabine (all $P < 0.05$). However, there were no significant differences between other chemotherapy drugs (paclitaxel and doxorubicin) and the risk score (Fig 10E and 10F). By analyzing data from the IMvigor210 trial (including 68 CR/PR patients and 230 SD/PD patients), we also found that the CR/PR rate in low-risk patients was higher than that in high-risk patients, which suggested that low-risk patients benefit significantly more from immunotherapy than high-risk patients (Fig 10G).

Table 3. Characteristics of the BC patients obtained from the GEO database.

Basic information		GSE32548 (n = 130)
Age		70 (median)
Gender	Female	31
	Male	99
Grade	G1	15
	G2	40
	G3	75
T classification	< T2	91
	≥ T2	38
	TX	1

BC, bladder cancer; GEO, Gene Expression Omnibus.

https://doi.org/10.1371/journal.pone.0264527.t003

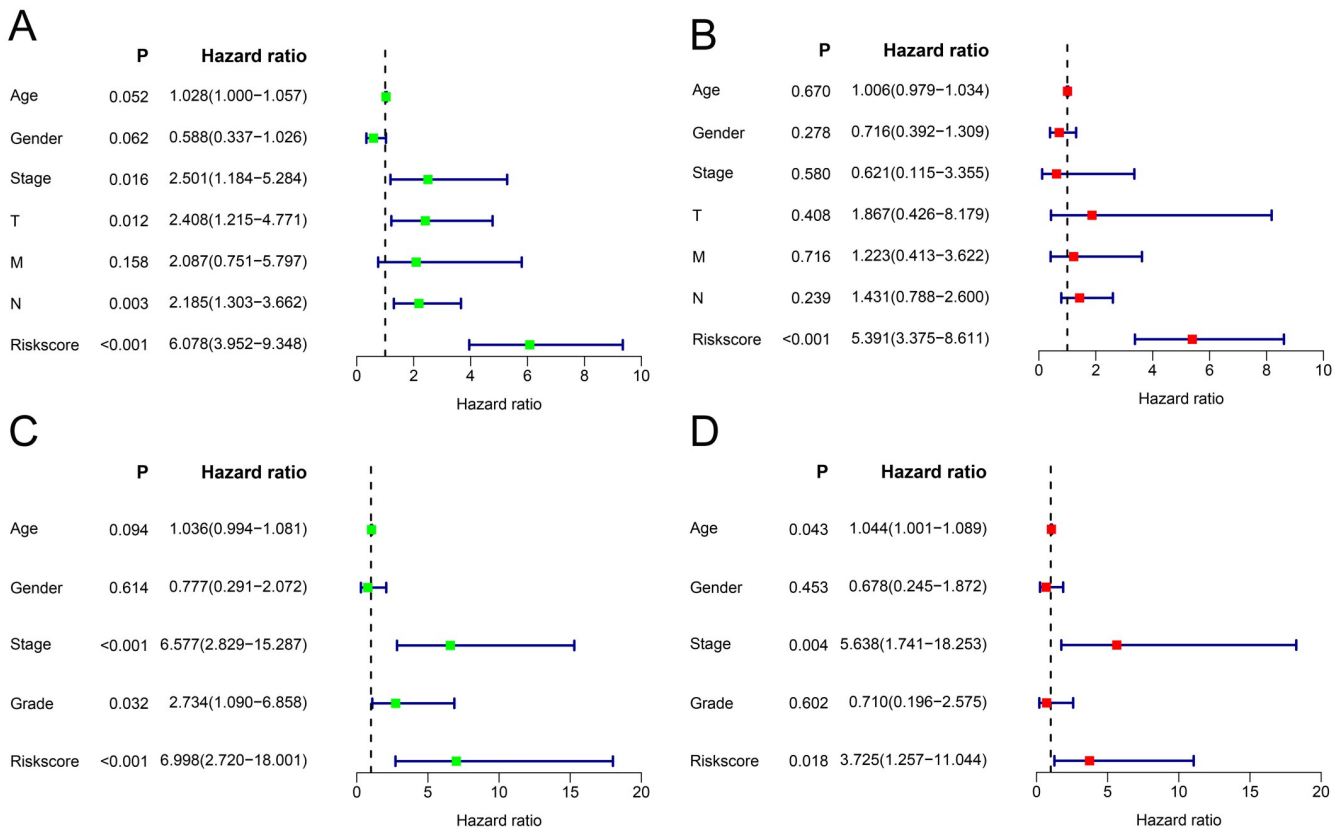

Fig 3. Independent prognostic analysis of the risk score. In the TCGA cohort, the results of univariate (A) and multivariate Cox analyses (B) showed that the risk score could be used as an independent prognostic factor for BC. In the GEO cohort, the results of univariate (C) and multivariate Cox analyses (D) also showed that the risk score could be used as an independent prognostic factor for BC. TCGA, The Cancer Genome Atlas; GEO, Gene Expression Omnibus; BC, bladder cancer.

https://doi.org/10.1371/journal.pone.0264527.g003

Analysis of biological functions

The biological functions of the risk score were evaluated via GSEA. The most significant biofunctions enriched in the high-risk group based on Gene Ontology (GO) and Kyoto Encyclopedia of Genes and Genomes (KEGG) analyses are listed in Tables 6 and 7, respectively. The most significant biofunctions enriched in the low-risk group based on KEGG analysis are listed in Table 8. Unfortunately, no significant pathways were found to be enriched in low-risk BC patients based on GO analyses.

Discussion

Currently, metabolic reprogramming, immune evasion and tumor-promoting inflammation are the three hallmarks of cancers [35]. As members of histone deacetylation metabolism, the role of HDACs in tumors has received widespread attention. As the HDAC IIa subtype, HDAC9 was found to play a dual role in tumors, which might be associated with the content of target proteins, alternative splicing, transcription factors that bind to the HDAC9 N-terminal region, and phosphorylation differences in multiple tumors [11, 36–39].

HDAC9 was initially found to be closely related to a variety of immunological parameters. And it was differentially expressed in five immune subtypes (previous research suggested that six immune subtypes could be identified in tumors, and there were significant differences in

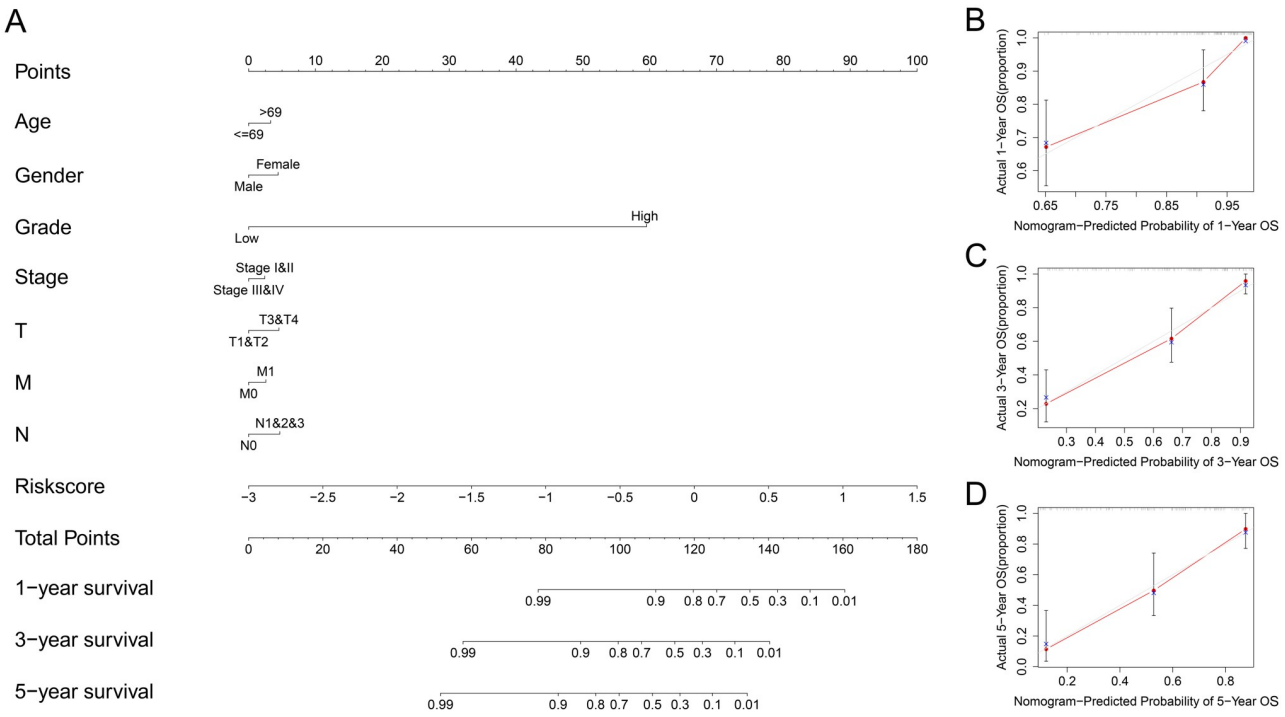

Fig 4. Establishment of the nomogram in TCGA. The results of the nomogram (A) and the calibration curve appropriately predicted 1-year (B), 3-year (C) and 5-year (D) OS for BC patients in TCGA. TCGA, The Cancer Genome Atlas; OS, overall survival; BC, bladder cancer.

https://doi.org/10.1371/journal.pone.0264527.g004

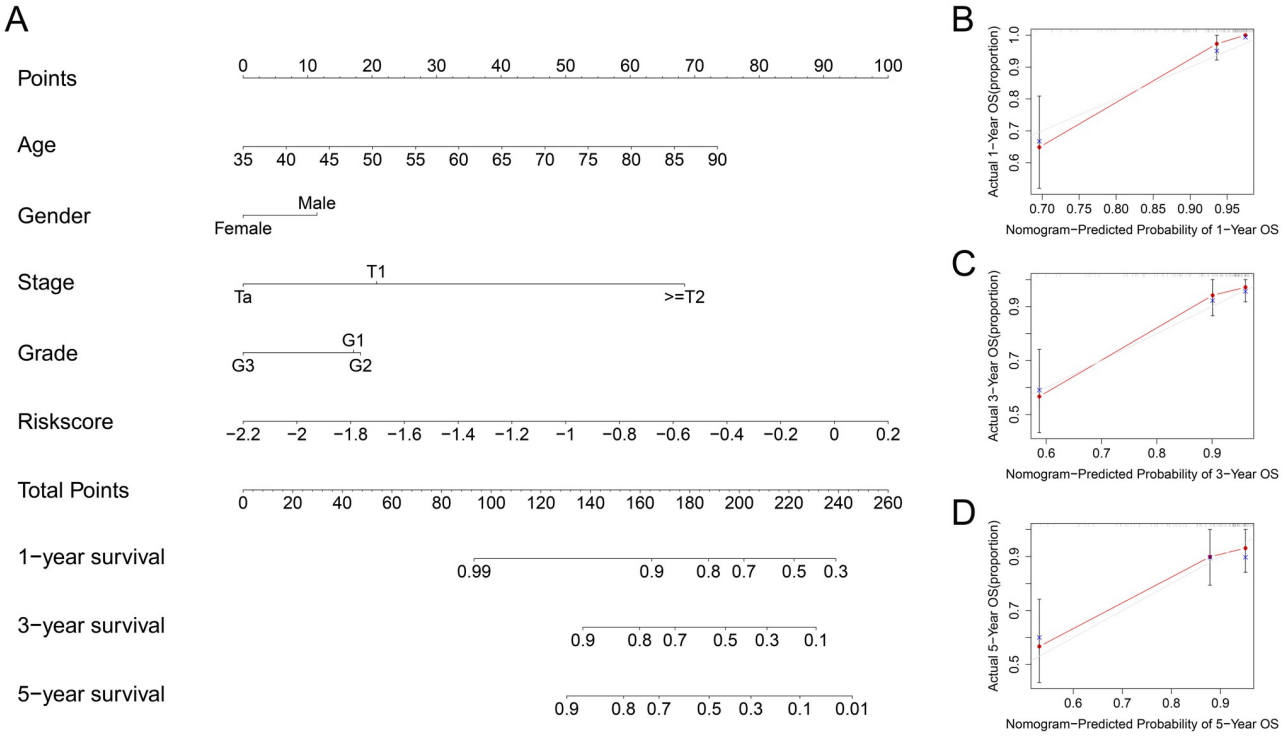

Fig 5. Establishment of the nomogram in GEO. The results of the nomogram (A) and the calibration curve appropriately predicted 1-year (B), 3-year (C) and 5-year (D) OS for BC patients in GEO. GEO, Gene Expression Omnibus; OS, overall survival; BC, bladder cancer.

https://doi.org/10.1371/journal.pone.0264527.g005

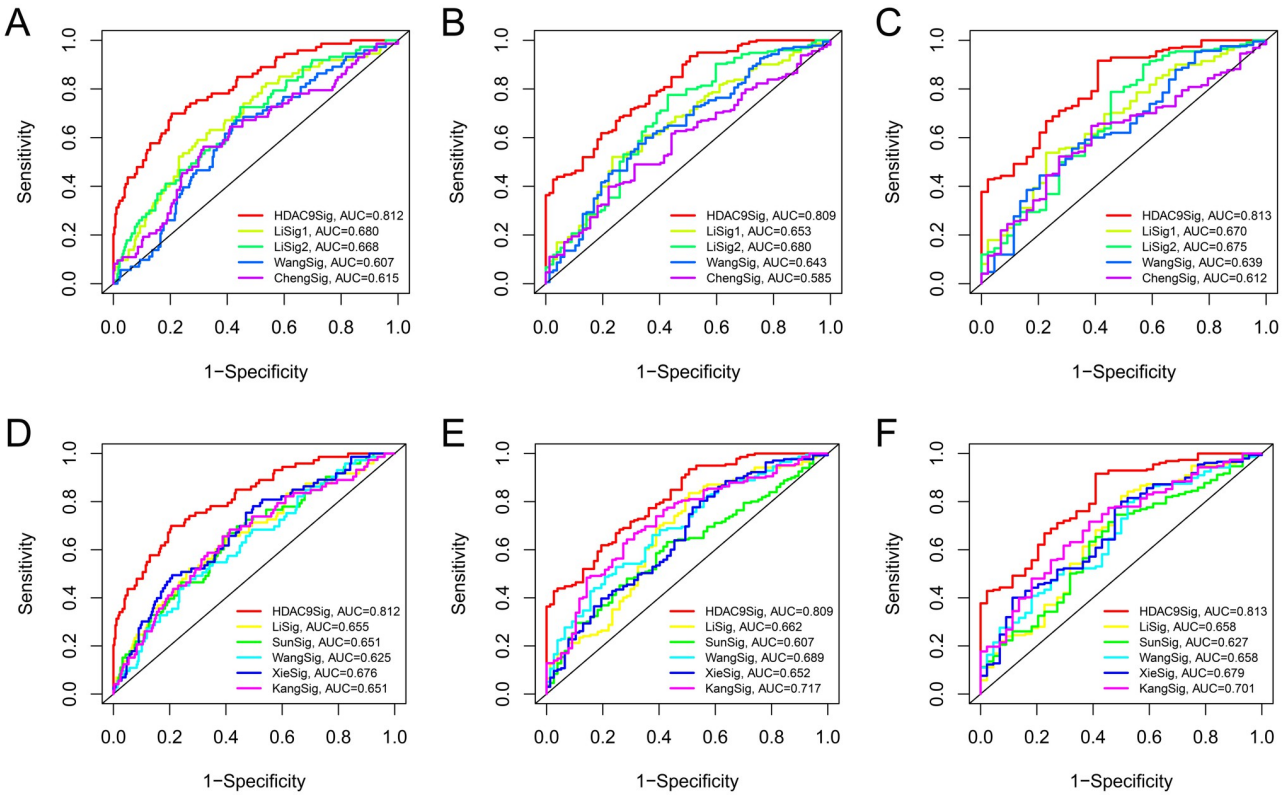

Fig 6. Comparison between signatures. By comparing with other signatures constructed through only prognostic-related genes (A-C) and other risk factors (D-F), our risk signature was found to be superior in performance.

https://doi.org/10.1371/journal.pone.0264527.g006

immune infiltration and sensitivity to immunotherapy among subtypes, five immune subtypes could be identified in BC) [34], implying that HDAC9 could be used to classify immune subtypes, which would help individualized treatment. However, further follow-up work is required to improve these results.

In our research, genes related to survival were identified from the top five enriched immune-related pathways based on the high expression status of HDAC9. Then, a risk signature using the selected genes was constructed. The high-risk group appeared to have a worse prognosis and be more sensitive to cisplatin and docetaxel. In contrast, low-risk BC patients were more sensitive to methotrexate and gemcitabine. Furthermore, low-risk patients had more significant benefits from immunotherapy.

Table 4. Comparison of ROC curve AUCs between HDAC9-associated immune-related signature and risk signatures based only on prognostic-related genes.

AUCs	1 year (P value)	3 years (P value)	5 years (P value)
HDAC9Sig vs LiSig1	0.001	0.000	0.002
HDAC9Sig vs LiSig2	0.001	0.003	0.017
HDAC9Sig vs WangSig	0.000	0.000	0.000
HDAC9Sig vs ChengSig	0.000	0.000	0.000

ROC, receiver operating characteristics; AUC, area under the curve; HDAC9, histone deacetylase 9; Sig, signature.

https://doi.org/10.1371/journal.pone.0264527.t004

Table 5. Comparison of ROC curve AUCs between HDAC9-associated immune-related signature and other risk signatures based on other risk factors.

AUCs	1 year (P value)	3 years (P value)	5 years (P value)
HDAC9Sig vs LiSig	0.000	0.000	0.003
HDAC9Sig vs SunSig	0.000	0.000	0.000
HDAC9Sig vs WangSig	0.000	0.002	0.001
HDAC9Sig vs XieSig	0.000	0.000	0.001
HDAC9Sig vs KangSig	0.000	0.012	0.013

ROC, receiver operating characteristics; AUC, area under the curve; HDAC9, histone deacetylase 9; Sig, signature.

https://doi.org/10.1371/journal.pone.0264527.t005

To date, six genes in the risk signature have been studied in relation to prognosis or TME in BC. Overexpression of LGALS1, MMP28, RNF26 and PHB could lead to poor clinical outcome of BC [40–43]. Increased KLRK1 expression was associated with better prognosis and was positively related to the activation of NK cells [44]. Decreased expression of PTPN6 suggested a poor prognosis and was connected with the infiltration of a variety of immune cells [45]. Interestingly, among the genes included in the risk signature, most were involved in metabolic processes. ANXA1, BCL6, CDK6, CLEC12B, FBXO7, FGR, GBP1, IRAK3, MMP28, NPLOC4, PTPN6, PTPRJ, RNF26, SUPT6H, TRIM27 and ZC3H8 participated in protein metabolism; BCL6, ZC3H8 and SUPT6H acted as transcriptional regulators [46–48]; MMP28 is a proteolysis factor [49]; ANXA1, CDK6, CLEC12B, FBXO7, FGR, GBP1, IRAK3, NPLOC4, PTPN6, PTPRJ, RNF26 and TRIM27 were involved in the posttranslational modification of proteins [45, 50–60]; ADIPOQ, ANGPT1, IL21, LDLR, OTOP1, ZBTB7B and ZC3H12A were closely related to lipid metabolism [61–67]; GPR68, IL12A, INS, KLRK1 and LGALS1 were

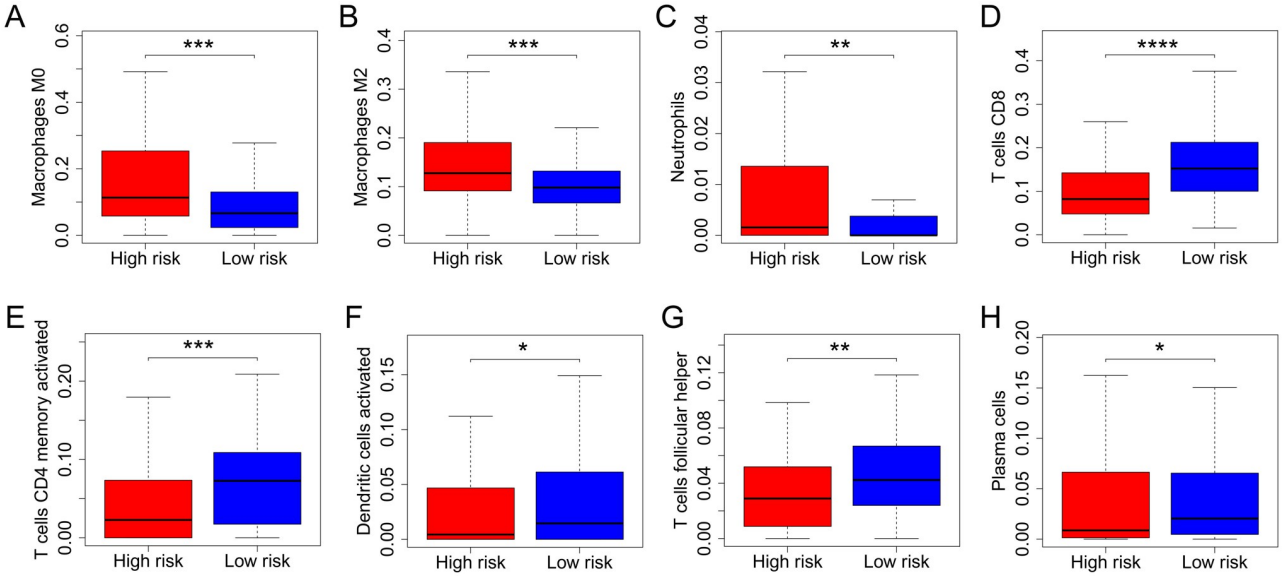

Fig 7. The risk score was associated with infiltration of various immune cells. The results of CIBERSORT indicated enrichment of signatures of M0 (A) and M2 macrophages (B) and neutrophils (C) in high-risk BC patients. Conversely, signatures of CD8 T cells (D), CD4 memory activated T cells (E), activated dendritic cells (F), follicular helper T cells (G) and plasma cells (H) were enriched in low-risk BC patients. CIBERSORT, cell type identification by estimating relative subsets of RNA transcripts; BC, bladder cancer; *, $P < 0.05$; **, $P < 0.01$; ***, $P < 0.001$.

https://doi.org/10.1371/journal.pone.0264527.g007

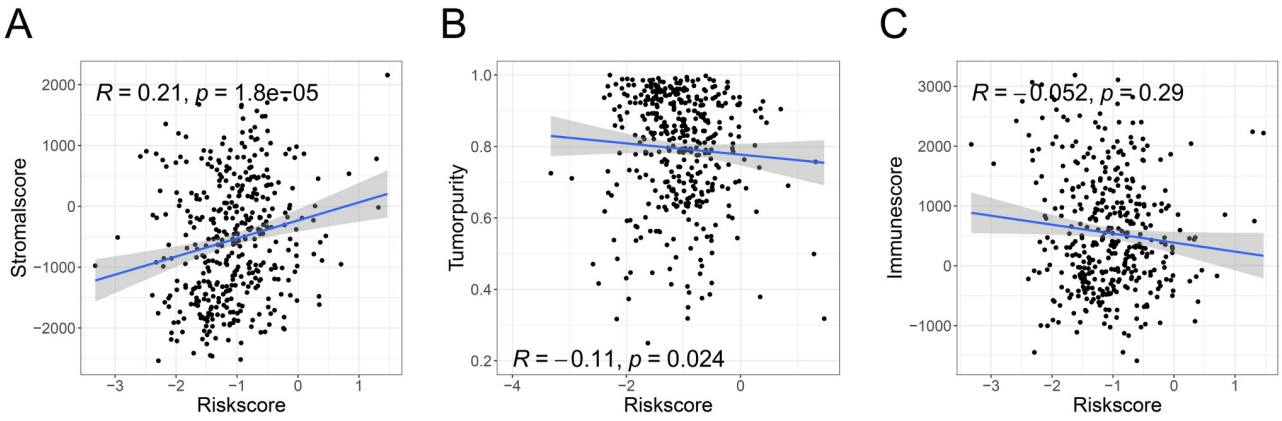

Fig 8. The risk score was significantly related to the TME based on the ESTIMATE algorithm. The stromal score was positively correlated with the risk score (A), and tumor purity was negatively correlated with the risk score (B). There was no significant difference between the risk score and immune score (C). TME, tumor microenvironment.

https://doi.org/10.1371/journal.pone.0264527.g008

found to regulate glucose metabolism [68–72]; MSH6 and TP53BP1 affected nucleotide metabolism by regulating DNA repair [73, 74]; and NR1H2 and PHB could simultaneously influence both glucose and lipid metabolism [75, 76]. Although immune-related pathways were activated under high HDAC9 expression, most enriched genes were metabolically related. In other words, changes in HDAC9, a regulator of protein posttranslational

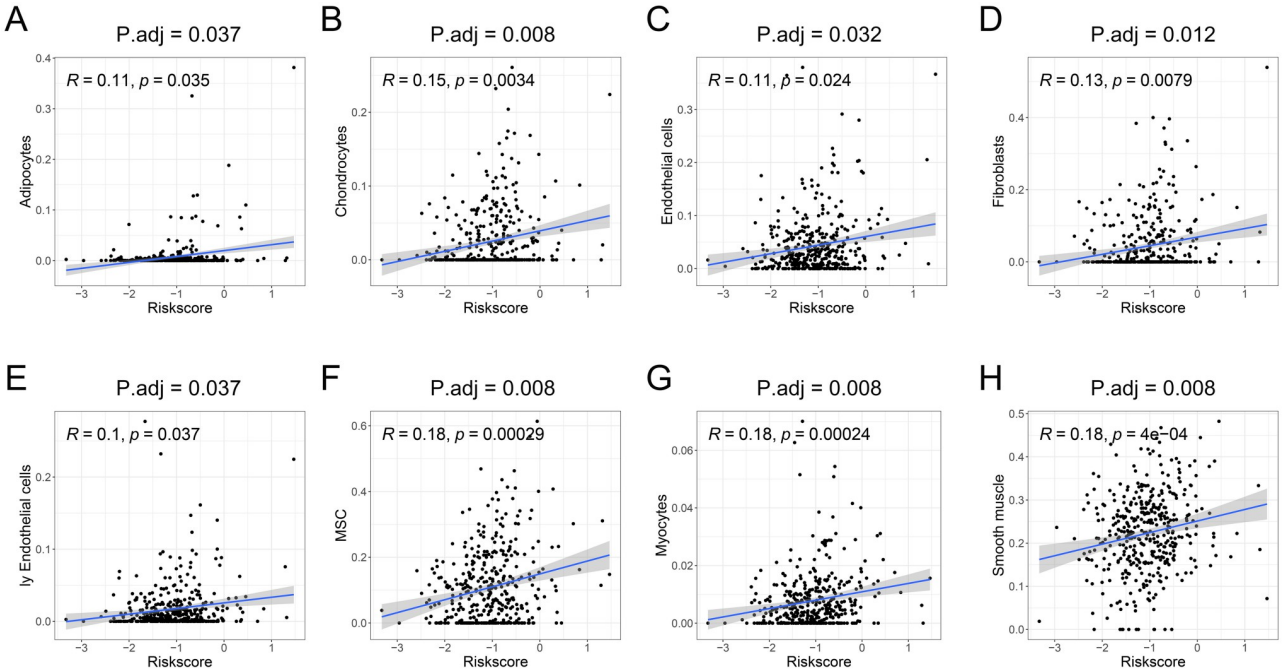

Fig 9. Stromal cells in BC patients based on the xCell algorithm. Results indicated that enrichment of signatures of eight stromal cells [adipocytes (A), chondrocytes (B), endothelial cells (C), fibroblasts (D), ly endothelial cells (E), MSCs (F), myocytes (G) and smooth muscle (H)] from the TME in the high-risk group. BC, bladder cancer; MSCs, mesenchymal stem cells; ly endothelial cells, lymphatic endothelial cells; TME, tumor microenvironment; P. adj, P. adjust.

https://doi.org/10.1371/journal.pone.0264527.g009

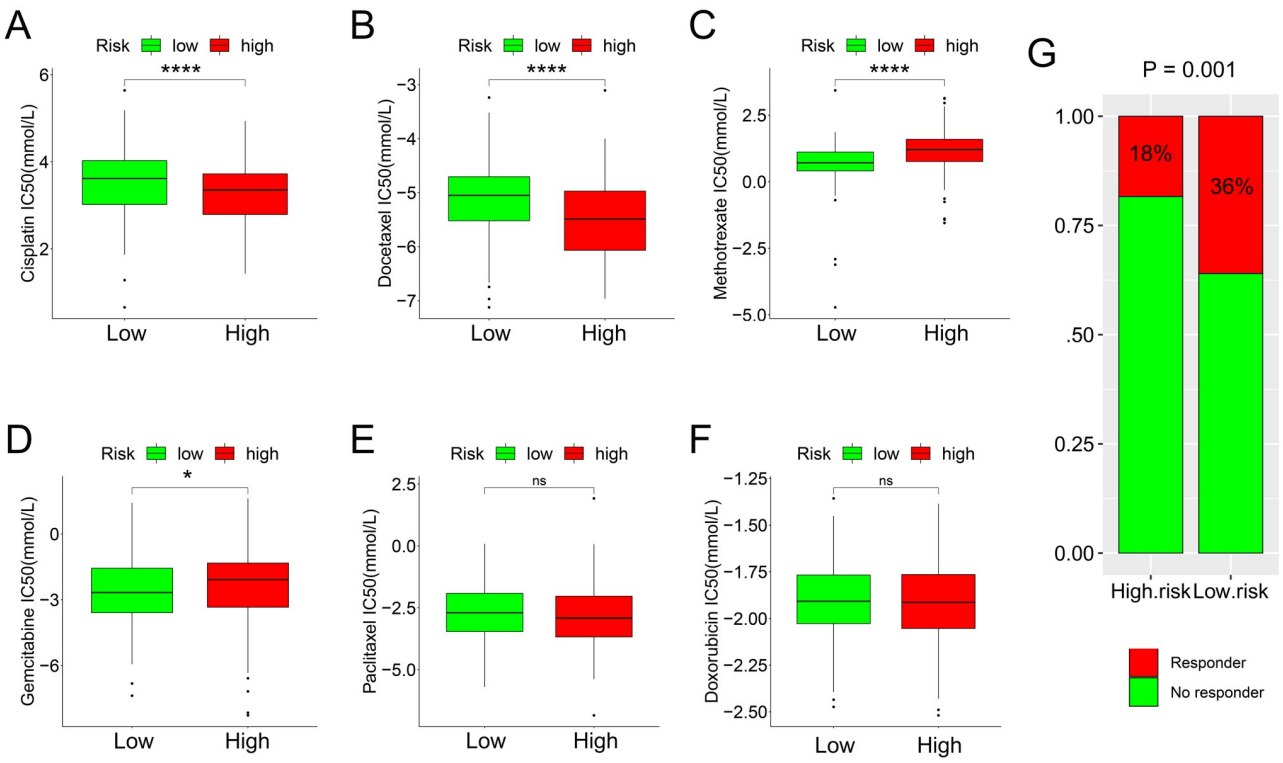

Fig 10. Risk score and drug sensitivity. Cisplatin (A) and docetaxel (B) exhibited higher IC50 values in low-risk patients; thus, the high-risk group was more sensitive to cisplatin and docetaxel. Methotrexate (C) and gemcitabine (D) exhibited a higher IC50 in high-risk BC patients; thus, low-risk BC patients were more sensitive to methotrexate and gemcitabine. However, there were no significant differences between other chemotherapy drugs (paclitaxel and doxorubicin) and the risk score (E-F). The CR/PR rate in low-risk patients was higher than that in high-risk patients (G), indicating more significant immunotherapy benefits for low-risk patients. IC50, half-maximal inhibitory concentration; SD, stable disease; PD, progressive disease; CR, complete response; PR, partial response; BC, bladder cancer; *, $P < 0.05$; ****, $P < 0.0001$.

https://doi.org/10.1371/journal.pone.0264527.g010

modifications, could potentially be connected to metabolic disorders. Metabolic disorders might lead to changes in HDAC9 expression and activity, or metabolism and HDAC9 could both be regulated by the same upstream signal; this will require rigorous biological experiments to verify. Therefore, immunity and metabolism were closely linked in BC. By observing the coexpression of HDAC9 and the genes included in the risk signature and the degree of difference, more potential factors could be selected for subsequent research.

By comparing with other risk signatures constructed only through prognosis-related genes, our risk signature was found to be superior in performance. One reason for this could be that the signature constructed by only prognosis-related genes was mixed with numerous factors that affect the prognosis of tumors (such as hypoxia and inflammation). The risk signature in our research used a metabolic factor (HDAC9) for stratification, and most of the immune-related genes included in the risk signature were related to various metabolic processes, which effectively reduced confounding factors. We focused on the influence of metabolic processes on BC. Interestingly, by comparing BC signatures constructed with other risk factors, the signature we built still had advantages, which indicated that the metabolic process in BC should attract attention.

The connection between the risk score and TME was further analyzed. The ESTIMATE results showed that the risk score was positively correlated with the stromal score and negatively correlated with tumor purity, and there was no significant difference between the risk

Table 6. Gene sets enriched in the high-risk phenotype via GO.

Gene set name	NES	NOM *p*-val	FDR *q*-val
GO_REGULATION_OF_CHONDROCYTE_DIFFERENTIATION	2.137	0.002	0.033
GO_SMOOTH_MUSCLE_CONTRACTION	2.131	0.000	0.030
GO_CONNECTIVE_TISSUE_DEVELOPMENT	2.115	0.000	0.029
GO_CELL_CELL_JUNCTION_ASSEMBLY	2.102	0.000	0.029
GO_POSITIVE_REGULATION_OF_CELL_DIVISION	2.099	0.000	0.029
GO_CELL_CELL_JUNCTION	2.095	0.000	0.030
GO_WNT_PROTEIN_BINDING	2.074	0.000	0.033
GO_TUBULIN_BINDING	2.059	0.000	0.029
GO_EPITHELIAL_TO_MESENCHYMAL_TRANSITION	2.034	0.000	0.034
GO_CHONDROCYTE_DEVELOPMENT	1.923	0.002	0.043
GO_FOLIC_ACID_METABOLIC_PROCESS	1.962	0.002	0.036
GO_POSITIVE_REGULATION_OF_ENDOTHELIAL_CELL_PROLIFERATION	1.916	0.004	0.044
GO_REGULATION_OF_GLUCOSE_TRANSMEMBRANE_TRANSPORT	1.905	0.004	0.044
GO_POSITIVE_REGULATION_OF_FIBROBLAST_MIGRATION	1.783	0.010	0.058
GO_ACTIVATION_OF_MAPK_ACTIVITY	1.762	0.026	0.061
GO_REGULATION_OF_STEROID_METABOLIC_PROCESS	1.733	0.006	0.068
GO_POSITIVE_REGULATION_OF_DNA_REPLICATION	1.694	0.048	0.076
GOBP_NEGATIVE_REGULATION_OF_CELL_CYCLE_G1_S_PHASE_TRANSITION	1.685	0.025	0.078
GO_CELLULAR_GLUCOSE_HOMEOSTASIS	1.656	0.000	0.084
GO_REGULATION_OF_LIPID_METABOLIC_PROCESS	1.638	0.041	0.086

GO, Gene Ontology; NES: normalized enrichment score; NOM: nominal; FDR: false discovery rate.
Gene sets with NOM p-val < 0.05 and FDR q-val < 0.25 were considered significant.

https://doi.org/10.1371/journal.pone.0264527.t006

Table 7. Gene sets enriched in the high-risk phenotype via KEGG.

Gene set name	NES	NOM *p*-val	FDR *q*-val
KEGG_ADHERENS_JUNCTION	2.069	0.002	0.012
KEGG_FOCAL_ADHESION	2.023	0.002	0.014
KEGG_ECM_RECEPTOR_INTERACTION	1.987	0.006	0.014
KEGG_TGF_BETA_SIGNALING_PATHWAY	1.941	0.000	0.019
KEGG_CELL_CYCLE	1.891	0.025	0.021
KEGG_WNT_SIGNALING_PATHWAY	2.090	0.000	0.023
KEGG_STEROID_BIOSYNTHESIS	1.819	0.016	0.040
KEGG_PURINE_METABOLISM	1.795	0.004	0.047
KEGG_VASCULAR_SMOOTH_MUSCLE_CONTRACTION	1.749	0.015	0.053
KEGG_GLYCOSAMINOGLYCAN_BIOSYNTHESIS_CHONDROITIN_SULFATE	1.696	0.036	0.062
KEGG_CYSTEINE_AND_METHIONINE_METABOLISM	1.644	0.039	0.077
KEGG_GLYCOLYSIS_GLUCONEOGENESIS	1.615	0.026	0.085
KEGG_MAPK_SIGNALING_PATHWAY	1.619	0.021	0.087
KEGG_SPHINGOLIPID_METABOLISM	1.558	0.045	0.101
KEGG_BLADDER_CANCER	1.543	0.036	0.108

KEGG, Kyoto Encyclopedia of Genes and Genomes; NES: normalized enrichment score; NOM: nominal; FDR: false discovery rate.
Gene sets with NOM p-val < 0.05 and FDR q-val < 0.25 were considered significant.

https://doi.org/10.1371/journal.pone.0264527.t007

Table 8. Gene sets enriched in the low-risk phenotype via KEGG.

ID	NES	NOM *p*-val	FDR *q*-val
KEGG_LINOLEIC_ACID_METABOLISM	-1.902	0.002	0.210
KEGG_RIG_I_LIKE_RECEPTOR_SIGNALING_PATHWAY	-1.841	0.012	0.179
KEGG_ARACHIDONIC_ACID_METABOLISM	-1.632	0.017	0.206

KEGG, Kyoto Encyclopedia of Genes and Genomes; NES: normalized enrichment score; NOM: nominal; FDR: false discovery rate.
Gene sets with NOM p-val < 0.05 and FDR q-val < 0.25 were considered significant.

https://doi.org/10.1371/journal.pone.0264527.t008

score and the immune score. However, the evaluation of specific immune cells through the CIBERSORT algorithm suggested that M0 and M2 macrophages and neutrophils were more enriched in the high-risk group, whereas CD8 T cells, activated memory CD4 T cells, follicular helper T cells, activated dendritic cells and plasma cells were more enriched in the low-risk group. M0 and M2 macrophages were positively correlated with a poor prognosis of BC [77, 78], while a higher infiltration level of CD8 T cells was correlated with a good prognosis [79, 80]. Therefore, the constructed risk score could appropriately assess immune cell infiltration, and it had an impact on immune cell infiltration. The lack of an association between overall immune score and risk score based on the ESTIMATE results suggested that the accumulation of negative effector immune cells in the high-risk group was close to that of positive effector immune cells in the low-risk group, resulting in no significant differences between the two groups. Additionally, the stromal score, which was significantly positively correlated with the risk score, could indicate that elevated stromal cells play an important role in different risk groups.

Through further analysis, enrichment of signatures of adipocytes, chondrocytes, endothelial cells, fibroblasts, ly endothelial cells, MSCs, myocytes, and smooth muscle was found in the high-risk BC patients. Studies have shown that adipocytes promote breast cancer metastasis [81] and that chondrocyte can promote the progression of tumors by secreting inflammatory factors [82]. By combining the results of ESTIMATE analysis, we hypothesize that the decrease in tumor purity due to the increased stromal cell infiltration might contribute to the poor prognosis of high-risk patients.

Chemotherapy is an important treatment for BC, and cisplatin is considered to be the first-line chemotherapy for advanced BC [83]. However, due to drug toxicity and heterogeneity among patients, 40–60% of patients with bladder cancer do not respond to cisplatin-based systemic chemotherapy [84, 85]. Studies have pointed out that the drug sensitivity of cisplatin in BC is closely related to ERKs and androgen receptors [86, 87]. Despite the existence of various cancer treatment strategies, chemotherapy drugs are still widely used. Due to drug resistance and side effects, the therapeutic effects of chemotherapeutic drugs are often very different and difficult to predict, and the risk score calculated by various related risk factors could be significantly related to drug sensitivity [88]. The risk signature we built could develop personalized treatments by stratifying the risks of BC patients. Adjusting the drug dosage and choosing anticancer treatment strategies according to individual specificities could improve the prognosis of patients and minimize side effects. The six chemotherapy drugs included in the study affected the metabolic process to varying degrees. Among the chemotherapeutic drugs with differences between the two risk groups, cisplatin could induce cell cycle G1/S arrest [89], docetaxel promoted the formation of tubulin structures [90], methotrexate prohibited folic acid metabolism [91] and gemcitabine inhibited DNA replication [92]. The GO results indicated G1/S cell cycle arrest (GOBP_NEGATIVE_REGULATION_OF_CELL_CYCLE_G1_S_PHASE_TRANSITION), tubulin structure synthesis (GO_TUBULIN_BINDING), folic acid

metabolism process (GO_FOLIC_ACID_METABOLIC_PROCESS), and the DNA replication (GO_POSITIVE_REGULATION_OF_DNA_REPLICATION) related biological functions were enriched in the high-risk group, implying that chemotherapy effectiveness depended on whether the drug mechanism conflicted with the metabolic changes of the patients themselves. If they conflicted (such as methotrexate and gemcitabine), the effectiveness would be reduced, and vice versa (such as cisplatin and docetaxel). Chemotherapeutic drugs with similar mechanisms may mainly act on different metabolic changes in patients selectively, which might eventually lead to the opposite results. These should be the content of subsequent in vivo and in vitro precise pharmacological experiments.

GSEA was conducted to explore biological mechanisms associated with the risk score. Based on GO analysis, a large number of stromal cells, junctions between cells and metabolic process-related biofunctions were significantly enriched in the high-risk BC patients. The results of KEGG revealed extracellular matrix (ECM), metabolic process and common BC-related pathways (WNT, TGF-β and MAPK pathways) to be enriched in the high-risk phenotype [93–98]. The ECM is crucial for maintaining tissue homeostasis, and its disruption can promote tumor occurrence, progression, and metastasis by inducing EMT [99–103]. Hence, the GO, KEGG, ESTIMATE and xCell results were consistent.

Finally, our research has some limitations. First, this research was retrospective in design, and due to the comparison of patients from different cohorts, heterogeneity existed. Therefore, it is necessary to verify the prospective cohort used in the future. Second, the results of GSEA stratified by HDAC9 status and TISIDB suggested that HDAC9 could play a dual role in immune function, and further analysis should be conducted to clarify the net effect of HDAC9 on immune function and related mechanisms in future studies. Third, the inherent molecular mechanism of the risk signature affecting the sensitivity of tumor chemotherapy drugs is worthy of in-depth exploration.

In summary, an immune-related prognostic signature based on HDAC9 expression that could independently predict BC patient prognosis was constructed. The genes included in this risk score may constitute new targets for the treatment of BC, and further study is warranted. Moreover, the use of this signature will help clinicians make personalized treatment decisions.

Supporting information

S1 Fig. The relationship between HDAC9 expression and TILs. The first six TILs with the strongest correlation with HDAC9 in BC were visualized (A-F). HDAC9, histone deacetylase 9; TILs, tumor-infiltrating lymphocytes; BC, bladder cancer.
(TIF)

S2 Fig. The relationship between HDAC9 expression and immunosuppressive cytokines. The first six immunosuppressive cytokines with the strongest correlation with HDAC9 in BC were visualized (A-F). HDAC9, histone deacetylase 9; BC, bladder cancer.
(TIF)

S3 Fig. The relationship between HDAC9 expression and immune-activating cytokines. The first six immune-activating cytokines with the strongest correlation with HDAC9 in BC were visualized (A-F). HDAC9, histone deacetylase 9; BC, bladder cancer.
(TIF)

S4 Fig. The relationship between HDAC9 expression and MHC molecules. The first six immune-activating cytokines with the strongest correlation with HDAC9 in BC were visualized (A-F). HDAC9, histone deacetylase 9; MHC, major histocompatibility complex; BC,

bladder cancer.
(TIF)

S5 Fig. Coexpression analysis. Coexpression analysis was performed to further understand connections between HDAC9 and the risk score genes. The relevant results were visualized via a heatmap. HDAC9, histone deacetylase 9; *, P. adjust <0.05; **, P. adjust < 0.01.
(TIF)

S6 Fig. The relationship between genes included in the risk signature and TME. Correlation analysis was performed to further understand connections between genes included in the risk signature and TME. The relevant results were visualized via a heatmap. TME, tumor microenvironment; *, P. adjust <0.05; **, P adjust < 0.01.
(TIF)

S1 Table. Genes related to survival were distinguished via univariable Cox regression.
(DOCX)

S2 Table. The coefficients of included genes.
(DOCX)

Author Contributions

Conceptualization: Jianbin Bi, Chuize Kong, Du Shi.

Data curation: Yang Fu, Shanshan Sun, Du Shi.

Formal analysis: Yang Fu, Shanshan Sun, Du Shi.

Funding acquisition: Chuize Kong.

Investigation: Yang Fu.

Methodology: Yang Fu, Jianbin Bi, Du Shi.

Project administration: Jianbin Bi, Chuize Kong.

Resources: Chuize Kong.

Software: Yang Fu, Shanshan Sun, Jianbin Bi.

Supervision: Yang Fu.

Validation: Yang Fu.

Visualization: Yang Fu.

Writing – original draft: Yang Fu, Shanshan Sun, Du Shi.

Writing – review & editing: Yang Fu, Shanshan Sun, Jianbin Bi, Chuize Kong, Du Shi.

References

1. Chen W, Zheng R, Baade PD, Zhang S, Zeng H, Bray F, et al. Cancer statistics in China, 2015. CA: a cancer journal for clinicians. 2016; 66(2):115–32. Epub 2016/01/26. https://doi.org/10.3322/caac.21338 PMID: 26808342.
2. von der Maase H, Hansen SW, Roberts JT, Dogliotti L, Oliver T, Moore MJ, et al. Gemcitabine and cisplatin versus methotrexate, vinblastine, doxorubicin, and cisplatin in advanced or metastatic bladder cancer: results of a large, randomized, multinational, multicenter, phase III study. J Clin Oncol. 2000; 18(17):3068–77. Epub 2000/09/23. https://doi.org/10.1200/JCO.2000.18.17.3068 PMID: 11001674.
3. Roberts JT, von der Maase H, Sengeløv L, Conte PF, Dogliotti L, Oliver T, et al. Long-term survival results of a randomized trial comparing gemcitabine/cisplatin and methotrexate/vinblastine/

doxorubicin/cisplatin in patients with locally advanced and metastatic bladder cancer. Annals of oncology: official journal of the European Society for Medical Oncology. 2006; 17 Suppl 5:v118–22. Epub 2006/06/30. https://doi.org/10.1093/annonc/mdj965 PMID: 16807438.

4. Antoni S, Ferlay J, Soerjomataram I, Znaor A, Jemal A, Bray F. Bladder Cancer Incidence and Mortality: A Global Overview and Recent Trends. Eur Urol. 2017; 71(1):96–108. Epub 2016/07/03. https://doi.org/10.1016/j.eururo.2016.06.010 PMID: 27370177.

5. Clocchiatti A, Florean C, Brancolini C. Class IIa HDACs: from important roles in differentiation to possible implications in tumourigenesis. J Cell Mol Med. 2011; 15(9):1833–46. Epub 2011/03/26. https://doi.org/10.1111/j.1582-4934.2011.01321.x PMID: 21435179.

6. Jin Z, Wei W, Huynh H, Wan Y. HDAC9 Inhibits Osteoclastogenesis via Mutual Suppression of PPARγ/RANKL Signaling. Molecular endocrinology (Baltimore, Md). 2015; 29(5):730–8. Epub 2015/03/21. https://doi.org/10.1210/me.2014-1365 PMID: 25793404.

7. Rosik L, Niegisch G, Fischer U, Jung M, Schulz WA, Hoffmann MJ. Limited efficacy of specific HDAC6 inhibition in urothelial cancer cells. Cancer biology & therapy. 2014; 15(6):742–57. Epub 2014/03/13. https://doi.org/10.4161/cbt.28469 PMID: 24618845.

8. Li H, Li X, Lin H, Gong J. High HDAC9 is associated with poor prognosis and promotes malignant progression in pancreatic ductal adenocarcinoma. Molecular medicine reports. 2020; 21(2):822–32. Epub 2020/01/25. https://doi.org/10.3892/mmr.2019.10869 PMID: 31974610.

9. Rastogi B, Raut SK, Panda NK, Rattan V, Radotra BD, Khullar M. Overexpression of HDAC9 promotes oral squamous cell carcinoma growth, regulates cell cycle progression, and inhibits apoptosis. Molecular and cellular biochemistry. 2016; 415(1–2):183–96. Epub 2016/03/20. https://doi.org/10.1007/s11010-016-2690-5 PMID: 26992905.

10. Salgado E, Bian X, Feng A, Shim H, Liang Z. HDAC9 overexpression confers invasive and angiogenic potential to triple negative breast cancer cells via modulating microRNA-206. Biochem Biophys Res Commun. 2018; 503(2):1087–91. Epub 2018/06/25. https://doi.org/10.1016/j.bbrc.2018.06.120 PMID: 29936177.

11. Yuan Z, Peng L, Radhakrishnan R, Seto E. Histone deacetylase 9 (HDAC9) regulates the functions of the ATDC (TRIM29) protein. The Journal of biological chemistry. 2010; 285(50):39329–38. Epub 2010/10/16. https://doi.org/10.1074/jbc.M110.179333 PMID: 20947501.

12. Xiong K, Zhang H, Du Y, Tian J, Ding S. Identification of HDAC9 as a viable therapeutic target for the treatment of gastric cancer. Experimental & molecular medicine. 2019; 51(8):1–15. Epub 2019/08/28. https://doi.org/10.1038/s12276-019-0301-8 PMID: 31451695.

13. Fu Y, Piao C, Zhang Z, Zhu Y, Sun S, Bi J, et al. Decreased expression and hypomethylation of HDAC9 lead to poor prognosis and inhibit immune cell infiltration in clear cell renal cell carcinoma. Urologic oncology. 2020; 38(9):740.e1–.e9. Epub 2020/05/14. https://doi.org/10.1016/j.urolonc.2020.03.006 PMID: 32402768.

14. Ning Y, Ding J, Sun X, Xie Y, Su M, Ma C, et al. HDAC9 deficiency promotes tumor progression by decreasing the CD8(+) dendritic cell infiltration of the tumor microenvironment. Journal for immunotherapy of cancer. 2020; 8(1). Epub 2020/06/20. https://doi.org/10.1136/jitc-2020-000529 PMID: 32554611.

15. Yan K, Cao Q, Reilly CM, Young NL, Garcia BA, Mishra N. Histone deacetylase 9 deficiency protects against effector T cell-mediated systemic autoimmunity. The Journal of biological chemistry. 2011; 286(33):28833–43. Epub 2011/06/29. https://doi.org/10.1074/jbc.M111.233932 PMID: 21708950.

16. Li X, Zhang Q, Ding Y, Liu Y, Zhao D, Zhao K, et al. Methyltransferase Dnmt3a upregulates HDAC9 to deacetylate the kinase TBK1 for activation of antiviral innate immunity. Nature immunology. 2016; 17(7):806–15. Epub 2016/05/31. https://doi.org/10.1038/ni.3464 PMID: 27240213.

17. Steinberg RL, Nepple KG, Velaer KN, Thomas LJ, O'Donnell MA. Quadruple immunotherapy of Bacillus Calmette-Guérin, interferon, interleukin-2, and granulocyte-macrophage colony-stimulating factor as salvage therapy for non-muscle-invasive bladder cancer. Urologic oncology. 2017; 35(12):670.e7–.e14. Epub 2017/08/13. https://doi.org/10.1016/j.urolonc.2017.07.024 PMID: 28801026.

18. Mariathasan S, Turley SJ, Nickles D, Castiglioni A, Yuen K, Wang Y, et al. TGFβ attenuates tumour response to PD-L1 blockade by contributing to exclusion of T cells. Nature. 2018; 554(7693):544–8. Epub 2018/02/15. https://doi.org/10.1038/nature25501 PMID: 29443960.

19. Ru B, Wong CN, Tong Y, Zhong JY, Zhong SSW, Wu WC, et al. TISIDB: an integrated repository portal for tumor-immune system interactions. Bioinformatics (Oxford, England). 2019; 35(20):4200–2. Epub 2019/03/25. https://doi.org/10.1093/bioinformatics/btz210 PMID: 30903160.

20. Li J, Cao J, Li P, Yao Z, Deng R, Ying L, et al. Construction of a novel mRNA-signature prediction model for prognosis of bladder cancer based on a statistical analysis. BMC Cancer. 2021; 21(1):858. Epub 2021/07/29. https://doi.org/10.1186/s12885-021-08611-z PMID: 34315402.

21. Li J, Lou Y, Li S, Sheng F, Liu S, Du E, et al. Identification and Immunocorrelation of Prognosis-Related Genes Associated With Development of Muscle-Invasive Bladder Cancer. Front Mol Biosci. 2020; 7:598599. Epub 2021/02/20. https://doi.org/10.3389/fmolb.2020.598599 PMID: 33604353.

22. Wang L, Shi J, Huang Y, Liu S, Zhang J, Ding H, et al. A six-gene prognostic model predicts overall survival in bladder cancer patients. Cancer Cell Int. 2019; 19:229. Epub 2019/09/14. https://doi.org/10.1186/s12935-019-0950-7 PMID: 31516386.

23. Cheng S, Jiang Z, Xiao J, Guo H, Wang Z, Wang Y. The prognostic value of six survival-related genes in bladder cancer. Cell Death Discov. 2020; 6:58. Epub 2020/07/23. https://doi.org/10.1038/s41420-020-00295-x PMID: 32695477.

24. Sun J, Yue W, You J, Wei X, Huang Y, Ling Z, et al. Identification of a Novel Ferroptosis-Related Gene Prognostic Signature in Bladder Cancer. Front Oncol. 2021; 11:730716. Epub 2021/09/25. https://doi.org/10.3389/fonc.2021.730716 PMID: 34557413.

25. Xie Z, Cai J, Sun W, Hua S, Wang X, Li A, et al. Development and Validation of Prognostic Model in Transitional Bladder Cancer Based on Inflammatory Response-Associated Genes. Front Oncol. 2021; 11:740985. Epub 2021/10/26. https://doi.org/10.3389/fonc.2021.740985 PMID: 34692520.

26. Li X, Fu S, Huang Y, Luan T, Wang H, Wang J. Identification of a novel metabolism-related gene signature associated with the survival of bladder cancer. BMC Cancer. 2021; 21(1):1267. Epub 2021/11/26. https://doi.org/10.1186/s12885-021-09006-w PMID: 34819038.

27. Wang Z, Tu L, Chen M, Tong S. Identification of a tumor microenvironment-related seven-gene signature for predicting prognosis in bladder cancer. BMC Cancer. 2021; 21(1):692. Epub 2021/06/12. https://doi.org/10.1186/s12885-021-08447-7 PMID: 34112144.

28. Kang Z, Li W, Yu YH, Che M, Yang ML, Len JJ, et al. Identification of Immune-Related Genes Associated With Bladder Cancer Based on Immunological Characteristics and Their Correlation With the Prognosis. Front Genet. 2021; 12:763590. Epub 2021/12/14. https://doi.org/10.3389/fgene.2021.763590 PMID: 34899848.

29. Newman AM, Liu CL, Green MR, Gentles AJ, Feng W, Xu Y, et al. Robust enumeration of cell subsets from tissue expression profiles. Nature methods. 2015; 12(5):453–7. Epub 2015/03/31. https://doi.org/10.1038/nmeth.3337 PMID: 25822800.

30. Yoshihara K, Shahmoradgoli M, Martinez E, Vegesna R, Kim H, Torres-Garcia W, et al. Inferring tumour purity and stromal and immune cell admixture from expression data. Nature communications. 2013; 4:2612. Epub 2013/10/12. https://doi.org/10.1038/ncomms3612 PMID: 24113773.

31. Aran D, Hu Z, Butte AJ. xCell: digitally portraying the tissue cellular heterogeneity landscape. Genome Biol. 2017; 18(1):220. Epub 2017/11/17. https://doi.org/10.1186/s13059-017-1349-1 PMID: 29141660 authors declare that they have no competing interests. PUBLISHER'S NOTE: Springer Nature remains neutral with regard to jurisdictional claims in published maps and institutional affiliations.

32. Geeleher P, Cox N, Huang RS. pRRophetic: an R package for prediction of clinical chemotherapeutic response from tumor gene expression levels. PLoS One. 2014; 9(9):e107468. Epub 2014/09/18. https://doi.org/10.1371/journal.pone.0107468 PMID: 25229481.

33. Blanche P, Dartigues JF, Jacqmin-Gadda H. Estimating and comparing time-dependent areas under receiver operating characteristic curves for censored event times with competing risks. Stat Med. 2013; 32(30):5381–97. Epub 2013/09/13. https://doi.org/10.1002/sim.5958 PMID: 24027076.

34. Thorsson V, Gibbs DL, Brown SD, Wolf D, Bortone DS, Ou Yang TH, et al. The Immune Landscape of Cancer. Immunity. 2019; 51(2):411–2. Epub 2019/08/23. https://doi.org/10.1016/j.immuni.2019.08.004 PMID: 31433971.

35. Li W, Xu M, Li Y, Huang Z, Zhou J, Zhao Q, et al. Comprehensive analysis of the association between tumor glycolysis and immune/inflammation function in breast cancer. J Transl Med. 2020; 18(1):92. Epub 2020/02/20. https://doi.org/10.1186/s12967-020-02267-2 PMID: 32070368.

36. Petrie K, Guidez F, Howell L, Healy L, Waxman S, Greaves M, et al. The histone deacetylase 9 gene encodes multiple protein isoforms. The Journal of biological chemistry. 2003; 278(18):16059–72. Epub 2003/02/19. https://doi.org/10.1074/jbc.M212935200 PMID: 12590135.

37. Li L, Yang XJ. Molecular and Functional Characterization of Histone Deacetylase 4 (HDAC4). Methods in molecular biology (Clifton, NJ). 2016; 1436:31–45. Epub 2016/06/02. https://doi.org/10.1007/978-1-4939-3667-0_4 PMID: 27246207.

38. Di Giorgio E, Brancolini C. Regulation of class IIa HDAC activities: it is not only matter of subcellular localization. Epigenomics. 2016; 8(2):251–69. Epub 2016/01/23. https://doi.org/10.2217/epi.15.106 PMID: 26791815.

39. Lucio-Eterovic AK, Cortez MA, Valera ET, Motta FJ, Queiroz RG, Machado HR, et al. Differential expression of 12 histone deacetylase (HDAC) genes in astrocytomas and normal brain tissue: class II and IV are hypoexpressed in glioblastomas. BMC cancer. 2008; 8:243. Epub 2008/08/21. https://doi.org/10.1186/1471-2407-8-243 PMID: 18713462.

40. Wu TF, Li CF, Chien LH, Shen KH, Huang HY, Su CC, et al. Galectin-1 dysregulation independently predicts disease specific survival in bladder urothelial carcinoma. J Urol. 2015; 193(3):1002–8. Epub 2014/10/07. https://doi.org/10.1016/j.juro.2014.09.107 PMID: 25284818.

41. Wang H, Wu JX, Chen XP, Zhang Q, Wei HB, Wang HJ, et al. Expression and Clinical Significance of MMP-28 in Bladder Cancer. Technol Cancer Res Treat. 2020; 19:1533033820974017. Epub 2020/11/17. https://doi.org/10.1177/1533033820974017 PMID: 33191847.

42. Yi L, Wang H, Li W, Ye K, Xiong W, Yu H, et al. The FOXM1/RNF26/p57 axis regulates the cell cycle to promote the aggressiveness of bladder cancer. Cell Death Dis. 2021; 12(10):944. Epub 2021/10/16. https://doi.org/10.1038/s41419-021-04260-z PMID: 34650035.

43. Wu TF, Wu H, Wang YW, Chang TY, Chan SH, Lin YP, et al. Prohibitin in the pathogenesis of transitional cell bladder cancer. Anticancer Res. 2007; 27(2):895–900. Epub 2007/05/01. PMID: 17465217.

44. Sun Y, Sedgwick AJ, Khan MA, Palarasah Y, Mangiola S, Barrow AD. A Transcriptional Signature of IL-2 Expanded Natural Killer Cells Predicts More Favorable Prognosis in Bladder Cancer. Front Immunol. 2021; 12:724107. Epub 2021/12/04. https://doi.org/10.3389/fimmu.2021.724107 PMID: 34858395.

45. Shen C, Liu J, Wang J, Yang X, Niu H, Wang Y. The Analysis of PTPN6 for Bladder Cancer: An Exploratory Study Based on TCGA. Dis Markers. 2020; 2020:4312629. Epub 2020/05/27. https://doi.org/10.1155/2020/4312629 PMID: 32454905.

46. Shaffer AL, Yu X, He Y, Boldrick J, Chan EP, Staudt LM. BCL-6 represses genes that function in lymphocyte differentiation, inflammation, and cell cycle control. Immunity. 2000; 13(2):199–212. Epub 2000/09/12. https://doi.org/10.1016/s1074-7613(00)00020-0 PMID: 10981963.

47. Bedi U, Scheel AH, Hennion M, Begus-Nahrmann Y, Rüschoff J, Johnsen SA. SUPT6H controls estrogen receptor activity and cellular differentiation by multiple epigenomic mechanisms. Oncogene. 2015; 34(4):465–73. Epub 2014/01/21. https://doi.org/10.1038/onc.2013.558 PMID: 24441044.

48. Hu D, Smith ER, Garruss AS, Mohaghegh N, Varberg JM, Lin C, et al. The little elongation complex functions at initiation and elongation phases of snRNA gene transcription. Mol Cell. 2013; 51(4):493–505. Epub 2013/08/13. https://doi.org/10.1016/j.molcel.2013.07.003 PMID: 23932780.

49. Zhou J, Zheng X, Feng M, Mo Z, Shan Y, Wang Y, et al. Upregulated MMP28 in Hepatocellular Carcinoma Promotes Metastasis via Notch3 Signaling and Predicts Unfavorable Prognosis. Int J Biol Sci. 2019; 15(4):812–25. Epub 2019/03/25. https://doi.org/10.7150/ijbs.31335 PMID: 30906212.

50. Ohnishi M, Tokuda M, Masaki T, Fujimura T, Tai Y, Itano T, et al. Involvement of annexin-I in glucose-induced insulin secretion in rat pancreatic islets. Endocrinology. 1995; 136(6):2421–6. Epub 1995/06/01. https://doi.org/10.1210/endo.136.6.7750463 PMID: 7750463.

51. Wang H, Nicolay BN, Chick JM, Gao X, Geng Y, Ren H, et al. The metabolic function of cyclin D3-CDK6 kinase in cancer cell survival. Nature. 2017; 546(7658):426–30. Epub 2017/06/14. https://doi.org/10.1038/nature22797 PMID: 28607489.

52. Chang YF, Cheng CM, Chang LK, Jong YJ, Yuo CY. The F-box protein Fbxo7 interacts with human inhibitor of apoptosis protein cIAP1 and promotes cIAP1 ubiquitination. Biochem Biophys Res Commun. 2006; 342(4):1022–6. Epub 2006/03/03. https://doi.org/10.1016/j.bbrc.2006.02.061 PMID: 16510124.

53. Acín-Pérez R, Iborra S, Martí-Mateos Y, Cook ECL, Conde-Garrosa R, Petcherski A, et al. Fgr kinase is required for proinflammatory macrophage activation during diet-induced obesity. Nat Metab. 2020; 2(9):974–88. Epub 2020/09/19. https://doi.org/10.1038/s42255-020-00273-8 PMID: 32943786.

54. Zhao J, Li X, Liu L, Cao J, Goscinski MA, Fan H, et al. Oncogenic Role of Guanylate Binding Protein 1 in Human Prostate Cancer. Front Oncol. 2019; 9:1494. Epub 2020/01/31. https://doi.org/10.3389/fonc.2019.01494 PMID: 31998647.

55. Wu X, Ouyang Y, Wang B, Lin J, Bai Y. Hypermethylation of the IRAK3-Activated MAPK Signaling Pathway to Promote the Development of Glioma. Cancer Manag Res. 2020; 12:7043–59. Epub 2020/08/28. https://doi.org/10.2147/CMAR.S252772 PMID: 32848462.

56. Hao Q, Jiao S, Shi Z, Li C, Meng X, Zhang Z, et al. A non-canonical role of the p97 complex in RIG-I antiviral signaling. Embo j. 2015; 34(23):2903–20. Epub 2015/10/17. https://doi.org/10.15252/embj.201591888 PMID: 26471729.

57. Spring K, Fournier P, Lapointe L, Chabot C, Roussy J, Pommey S, et al. The protein tyrosine phosphatase DEP-1/PTPRJ promotes breast cancer cell invasion and metastasis. Oncogene. 2015; 34(44):5536–47. Epub 2015/03/17. https://doi.org/10.1038/onc.2015.9 PMID: 25772245.

58. Ma L, Yao N, Chen P, Zhuang Z. TRIM27 promotes the development of esophagus cancer via regulating PTEN/AKT signaling pathway. Cancer Cell Int. 2019; 19:283. Epub 2019/11/14. https://doi.org/10.1186/s12935-019-0998-4 PMID: 31719796.

59. Hoffmann SC, Schellack C, Textor S, Konold S, Schmitz D, Cerwenka A, et al. Identification of CLEC12B, an inhibitory receptor on myeloid cells. J Biol Chem. 2007; 282(31):22370–5. Epub 2007/06/15. https://doi.org/10.1074/jbc.M704250200 PMID: 17562706.

60. Qin Y, Zhou MT, Hu MM, Hu YH, Zhang J, Guo L, et al. RNF26 temporally regulates virus-triggered type I interferon induction by two distinct mechanisms. PLoS Pathog. 2014; 10(9):e1004358. Epub 2014/09/26. https://doi.org/10.1371/journal.ppat.1004358 PMID: 25254379.

61. Parida S, Siddharth S, Sharma D. Adiponectin, Obesity, and Cancer: Clash of the Bigwigs in Health and Disease. Int J Mol Sci. 2019; 20(10). Epub 2019/05/28. https://doi.org/10.3390/ijms20102519 PMID: 31121868.

62. Go GW, Mani A. Low-density lipoprotein receptor (LDLR) family orchestrates cholesterol homeostasis. The Yale journal of biology and medicine. 2012; 85(1):19–28. Epub 2012/03/31. PMID: 22461740.

63. Ehrlich KC, Lacey M, Ehrlich M. Tissue-specific epigenetics of atherosclerosis-related ANGPT and ANGPTL genes. Epigenomics. 2019; 11(2):169–86. Epub 2019/01/29. https://doi.org/10.2217/epi-2018-0150 PMID: 30688091.

64. Knudsen NH, Lee CH. IL-21 and IRF4: A complex partnership in immune and metabolic regulation. Diabetes. 2014; 63(6):1838–40. Epub 2014/05/24. https://doi.org/10.2337/db14-0273 PMID: 24853897.

65. Li S, Mi L, Yu L, Yu Q, Liu T, Wang GX, et al. Zbtb7b engages the long noncoding RNA Blnc1 to drive brown and beige fat development and thermogenesis. Proc Natl Acad Sci U S A. 2017; 114(34): E7111–e20. Epub 2017/08/09. https://doi.org/10.1073/pnas.1703494114 PMID: 28784777.

66. Losko M, Dolicka D, Pydyn N, Jankowska U, Kedracka-Krok S, Kulecka M, et al. Integrative genomics reveal a role for MCPIP1 in adipogenesis and adipocyte metabolism. Cell Mol Life Sci. 2020; 77 (23):4899–919. Epub 2020/01/02. https://doi.org/10.1007/s00018-019-03434-5 PMID: 31893310.

67. Wang GX, Cho KW, Uhm M, Hu CR, Li S, Cozacov Z, et al. Otopetrin 1 protects mice from obesity-associated metabolic dysfunction through attenuating adipose tissue inflammation. Diabetes. 2014; 63 (4):1340–52. Epub 2014/01/01. https://doi.org/10.2337/db13-1139 PMID: 24379350.

68. Wiley SZ, Sriram K, Salmerón C, Insel PA. GPR68: An Emerging Drug Target in Cancer. Int J Mol Sci. 2019; 20(3). Epub 2019/01/31. https://doi.org/10.3390/ijms20030559 PMID: 30696114.

69. Kochumon S, Al Madhoun A, Al-Rashed F, Thomas R, Sindhu S, Al-Ozairi E, et al. Elevated adipose tissue associated IL-2 expression in obesity correlates with metabolic inflammation and insulin resistance. Sci Rep. 2020; 10(1):16364. Epub 2020/10/03. https://doi.org/10.1038/s41598-020-73347-y PMID: 33004937.

70. Tager H, Given B, Baldwin D, Mako M, Markese J, Rubenstein A, et al. A structurally abnormal insulin causing human diabetes. Nature. 1979; 281(5727):122–5. Epub 1979/09/13. https://doi.org/10.1038/281122a0 PMID: 381941.

71. Xia M, Guerra N, Sukhova GK, Yang K, Miller CK, Shi GP, et al. Immune activation resulting from NKG2D/ligand interaction promotes atherosclerosis. Circulation. 2011; 124(25):2933–43. Epub 2011/11/23. https://doi.org/10.1161/CIRCULATIONAHA.111.034850 PMID: 22104546.

72. Blois SM, Gueuvoghlanian-Silva BY, Tirado-González I, Torloni MR, Freitag N, Mattar R, et al. Getting too sweet: galectin-1 dysregulation in gestational diabetes mellitus. Mol Hum Reprod. 2014; 20 (7):644–9. Epub 2014/03/19. https://doi.org/10.1093/molehr/gau021 PMID: 24637109.

73. Thirumal Kumar D, Susmita B, Judith E, Priyadharshini Christy J, George Priya Doss C, Zayed H. Elucidating the role of interacting residues of the MSH2-MSH6 complex in DNA repair mechanism: A computational approach. Advances in protein chemistry and structural biology. 2019; 115:325–50. Epub 2019/02/26. https://doi.org/10.1016/bs.apcsb.2018.11.005 PMID: 30798936.

74. Guo G, Li L, Song G, Wang J, Yan Y, Zhao Y. miR-7/SP1/TP53BP1 axis may play a pivotal role in NSCLC radiosensitivity. Oncol Rep. 2020; 44(6):2678–90. Epub 2020/10/31. https://doi.org/10.3892/or.2020.7824 PMID: 33125142.

75. Mishra S, Nyomba BG. Prohibitin—At the crossroads of obesity-linked diabetes and cancer. Exp Biol Med (Maywood). 2017; 242(11):1170–7. Epub 2017/04/13. https://doi.org/10.1177/1535370217703976 PMID: 28399645.

76. Rooki H, Ghayour-Mobarhan M, Haerian MS, Ebrahimi M, Azimzadeh P, Heidari-Bakavoli A, et al. Lack of association between LXRα and LXRβ gene polymorphisms and prevalence of metabolic syndrome: a case-control study of an Iranian population. Gene. 2013; 532(2):288–93. Epub 2013/10/09. https://doi.org/10.1016/j.gene.2013.09.107 PMID: 24100084.

77. Liu J, Duan X. PA-MSHA induces apoptosis and suppresses metastasis by tumor associated macrophages in bladder cancer cells. Cancer Cell Int. 2017; 17:76. Epub 2017/08/22. https://doi.org/10.1186/s12935-017-0445-3 PMID: 28824336.

78. Li W, Zeng J, Luo B, Mao Y, Liang Y, Zhao W, et al. [High expression of activated CD4(+) memory T cells and CD8(+) T cells and low expression of M0 macrophage are associated with better clinical prognosis in bladder cancer patients]. Xi Bao Yu Fen Zi Mian Yi Xue Za Zhi. 2020; 36(2):97–103. Epub 2020/04/22. PMID: 32314705.

79. Hartana CA, Ahlén Bergman E, Zirakzadeh AA, Krantz D, Winerdal ME, Winerdal M, et al. Urothelial bladder cancer may suppress perforin expression in CD8+ T cells by an ICAM-1/TGFβ2 mediated pathway. PLoS One. 2018; 13(7):e0200079. Epub 2018/07/03. https://doi.org/10.1371/journal.pone.0200079 PMID: 29966014.

80. Oh DY, Kwek SS, Raju SS, Li T, McCarthy E, Chow E, et al. Intratumoral CD4(+) T Cells Mediate Anti-tumor Cytotoxicity in Human Bladder Cancer. Cell. 2020; 181(7):1612–25.e13. Epub 2020/06/05. https://doi.org/10.1016/j.cell.2020.05.017 PMID: 32497499.

81. Li J, Han X. Adipocytokines and breast cancer. Current problems in cancer. 2018; 42(2):208–14. Epub 2018/02/13. https://doi.org/10.1016/j.currproblcancer.2018.01.004 PMID: 29433827.

82. Qiu S, Deng L, Liao X, Nie L, Qi F, Jin K, et al. Tumor-associated macrophages promote bladder tumor growth through PI3K/AKT signal induced by collagen. Cancer science. 2019; 110(7):2110–8. Epub 2019/05/24. https://doi.org/10.1111/cas.14078 PMID: 31120174.

83. Wang D, Chen Z, Lin F, Wang Z, Gao Q, Xie H, et al. OIP5 Promotes Growth, Metastasis and Chemoresistance to Cisplatin in Bladder Cancer Cells. J Cancer. 2018; 9(24):4684–95. Epub 2018/12/28. https://doi.org/10.7150/jca.27381 PMID: 30588253.

84. Voskuilen CS, Oo HZ, Genitsch V, Smit LA, Vidal A, Meneses M, et al. Multicenter Validation of Histopathologic Tumor Regression Grade After Neoadjuvant Chemotherapy in Muscle-invasive Bladder Carcinoma. Am J Surg Pathol. 2019; 43(12):1600–10. Epub 2019/09/17. https://doi.org/10.1097/PAS.0000000000001371 PMID: 31524642.

85. Zargar H, Espiritu PN, Fairey AS, Mertens LS, Dinney CP, Mir MC, et al. Multicenter assessment of neoadjuvant chemotherapy for muscle-invasive bladder cancer. Eur Urol. 2015; 67(2):241–9. Epub 2014/09/27. https://doi.org/10.1016/j.eururo.2014.09.007 PMID: 25257030.

86. Kashiwagi E, Inoue S, Mizushima T, Chen J, Ide H, Kawahara T, et al. Prostaglandin receptors induce urothelial tumourigenesis as well as bladder cancer progression and cisplatin resistance presumably via modulating PTEN expression. Br J Cancer. 2018; 118(2):213–23. Epub 2017/11/11. https://doi.org/10.1038/bjc.2017.393 PMID: 29123257.

87. Teramoto Y, Jiang G, Goto T, Mizushima T, Nagata Y, Netto GJ, et al. Androgen Receptor Signaling Induces Cisplatin Resistance via Down-Regulating GULP1 Expression in Bladder Cancer. Int J Mol Sci. 2021; 22(18). Epub 2021/09/29. https://doi.org/10.3390/ijms221810030 PMID: 34576193.

88. Tan G, Wu A, Li Z, Chen G, Wu Y, Huang S, et al. Bioinformatics analysis based on immune-autophagy-related lncRNAs combined with immune infiltration in bladder cancer. Transl Androl Urol. 2021; 10(8):3440–55. Epub 2021/09/18. https://doi.org/10.21037/tau-21-560 PMID: 34532269.

89. Gao X, Kong L, Lu X, Zhang G, Chi L, Jiang Y, et al. Paraspeckle protein 1 (PSPC1) is involved in the cisplatin induced DNA damage response—role in G1/S checkpoint. PLoS One. 2014; 9(5):e97174. Epub 2014/05/14. https://doi.org/10.1371/journal.pone.0097174 PMID: 24819514 Testing International Corporation", it does not alter the authors adherence to PLOS ONE policies on sharing data and materials.

90. Chen X, Winstead A, Yu H, Peng J. Taccalonolides: A Novel Class of Microtubule-Stabilizing Anticancer Agents. Cancers (Basel). 2021; 13(4). Epub 2021/03/07. https://doi.org/10.3390/cancers13040920 PMID: 33671665.

91. Ravaei A, Rubini M. Rescuing effect of folates on methotrexate cytotoxicity in human trophoblast cells. Clin Exp Rheumatol. 2021. Epub 2021/10/20. PMID: 34665710.

92. Shewach DS, Lawrence TS. Gemcitabine and radiosensitization in human tumor cells. Invest New Drugs. 1996; 14(3):257–63. Epub 1996/01/01. https://doi.org/10.1007/BF00194528 PMID: 8958180.

93. Lv D, Wu H, Xing R, Shu F, Lei B, Lei C, et al. HnRNP-L mediates bladder cancer progression by inhibiting apoptotic signaling and enhancing MAPK signaling pathways. Oncotarget. 2017; 8(8):13586–99. Epub 2017/01/16. https://doi.org/10.18632/oncotarget.14600 PMID: 28088793.

94. Sun M, Zhao W, Chen Z, Li M, Li S, Wu B, et al. Circular RNA CEP128 promotes bladder cancer progression by regulating Mir-145-5p/Myd88 via MAPK signaling pathway. International journal of cancer. 2019; 145(8):2170–81. Epub 2019/04/03. https://doi.org/10.1002/ijc.32311 PMID: 30939216.

95. Chen Z, He S, Zhan Y, He A, Fang D, Gong Y, et al. TGF-β-induced transgelin promotes bladder cancer metastasis by regulating epithelial-mesenchymal transition and invadopodia formation. EBioMedicine. 2019; 47:208–20. Epub 2019/08/20. https://doi.org/10.1016/j.ebiom.2019.08.012 PMID: 31420300.

96. Yang HJ, Liu GL, Liu B, Liu T. GP73 promotes invasion and metastasis of bladder cancer by regulating the epithelial-mesenchymal transition through the TGF-β1/Smad2 signalling pathway. J Cell Mol Med. 2018; 22(3):1650–65. Epub 2018/01/20. https://doi.org/10.1111/jcmm.13442 PMID: 29349903.

97. Yang R, Liao Z, Cai Y, Kong J. LASP2 suppressed malignancy and Wnt/β-catenin signaling pathway activation in bladder cancer. Experimental and therapeutic medicine. 2018; 16(6):5215–23. Epub 2018/12/14. https://doi.org/10.3892/etm.2018.6836 PMID: 30542477.

98. Pang G, Xie Q, Yao J. Mitofusin 2 inhibits bladder cancer cell proliferation and invasion via the Wnt/β-catenin pathway. Oncology letters. 2019; 18(3):2434–42. Epub 2019/08/14. https://doi.org/10.3892/ol.2019.10570 PMID: 31402945.

99. Luo Y, Zeng G, Wu S. Identification of Microenvironment-Related Prognostic Genes in Bladder Cancer Based on Gene Expression Profile. Frontiers in genetics. 2019; 10:1187. Epub 2019/12/12. https://doi.org/10.3389/fgene.2019.01187 PMID: 31824575.

100. Shintani Y, Hollingsworth MA, Wheelock MJ, Johnson KR. Collagen I promotes metastasis in pancreatic cancer by activating c-Jun NH(2)-terminal kinase 1 and up-regulating N-cadherin expression. Cancer Res. 2006; 66(24):11745–53. Epub 2006/12/21. https://doi.org/10.1158/0008-5472.CAN-06-2322 PMID: 17178870.

101. Torzilli PA, Bourne JW, Cigler T, Vincent CT. A new paradigm for mechanobiological mechanisms in tumor metastasis. Seminars in cancer biology. 2012; 22(5–6):385–95. Epub 2012/05/23. https://doi.org/10.1016/j.semcancer.2012.05.002 PMID: 22613484.

102. Quail DF, Joyce JA. Microenvironmental regulation of tumor progression and metastasis. Nature medicine. 2013; 19(11):1423–37. Epub 2013/11/10. https://doi.org/10.1038/nm.3394 PMID: 24202395.

103. Hynes RO. The extracellular matrix: not just pretty fibrils. Science (New York, NY). 2009; 326 (5957):1216–9. Epub 2009/12/08. https://doi.org/10.1126/science.1176009 PMID: 19965464.